Schizophrenia

REVIEW ARTICLE   OPEN

Early-stage visual perception impairment in schizophrenia, bottom-up and back again

Petr Adámek [ID][1,2 ✉], Veronika Langová[1,2] and Jiří Horáček[1,2]

Visual perception is one of the basic tools for exploring the world. However, in schizophrenia, this modality is disrupted. So far, there has been no clear answer as to whether the disruption occurs primarily within the brain or in the precortical areas of visual perception (the retina, visual pathways, and lateral geniculate nucleus [LGN]). A web-based comprehensive search of peer-reviewed journals was conducted based on various keyword combinations including schizophrenia, saliency, visual cognition, visual pathways, retina, and LGN. Articles were chosen with respect to topic relevance. Searched databases included Google Scholar, PubMed, and Web of Science. This review describes the precortical circuit and the key changes in biochemistry and pathophysiology that affect the creation and characteristics of the retinal signal as well as its subsequent modulation and processing in other parts of this circuit. Changes in the characteristics of the signal and the misinterpretation of visual stimuli associated with them may, as a result, contribute to the development of schizophrenic disease.

INTRODUCTION

Schizophrenia affects a wide range of domains within information processing such as perception, thinking, attention, verbal fluency, working memory, executive functions, verbal memory, and learning[1]. These changes affect even the initial phase of information processing—perception, which is one of the fundamental tools humans use to learn about the world and adapt to its conditions. A disruption of the mechanisms involved in the processing of all perception modalities—olfactory[2], somatosensoric[3], auditory[4,5], and visual percepts[4,6–8]—has been repeatedly demonstrated in schizophrenia.

Changes in visual perception in schizophrenia patients are apparent at the level of the oculomotor response to visual stimuli[9–11]. These disruptions also manifest as abnormalities in perceptional organization[12], sensitivity to contrasts[7,13], inaccurate perception of motion[14], colors, brightness, distortion of shapes, and the disruption of perception of human figures and their emotional expressions[15]. These changes in visual perception are evident not only during acute schizophrenia episodes, but also in patients in remission[3,16], and some may also be found in their relatives[17–19]. Congruently, longitudinal studies have shown the possibility to selectively predict the development of schizophrenia spectrum disorders in early adults based on measurements of the dysfunction rate in visual perception tasks performed by a high-risk child population[20,21]. Abnormalities of visual perception may, therefore, be considered as endophenotypes of schizophrenia[22,23].

The incidence of disruption of visual perception in schizophrenia patients is high, ranging between 40 and 62%[24], and has been described in the prodromal stage of the disorder[25]. Current views attribute impaired efficiency/functionality in visual perception processing in schizophrenia patients mainly to dopaminergic modulation of the incoming signal. This modulation is related to gain control and its subsequent integration into visual processing[26].

One characteristic impairment is instability in the ability to process low spatial frequency (LSF) information from a visual scene. LSF information is rapidly extracted from a visual stimulus and provides general information about the shape and orientation of objects in a visual scene. Top-down prediction, which affects our visual attention and higher brain functions related to visual cognition, is then formed based on these LSF data[27–30]. In early-stage and untreated first-episode patients, hypersensitivity is often encountered, which eventually progresses to hyposensitivity, which also begins to extend to other frequencies of the visual scene[26,31,32]. The impairment of sensitivity to spatial frequencies is not limited to LSFs, however, and as the disease progresses, it begins to manifest in the middle and high spatial frequencies as well. LSFs probably occupy a specific place within visual information processing[28].

One of the main consequences of the disruption of this process is a disorder of attention and the inability to integrate salient percepts into the stream of consciousness[33,34]. In schizophrenia, the occurrence of brain activation abnormalities (both hyper- and hypoactivations) in visual tasks has been described in temporal[35], occipital[36,37], parietal, and prefrontal[38,39] areas, depending on specific experimental tasks. These tasks reflect both the disruption of the mechanisms of basal visual perception based on incorrect processing of visual stimuli (bottom-up)[7,13,37,40] and the disruption of higher visual cognition based on the processing of visual stimuli influenced and orchestrated by previous experience (top-down/feedforward sweep)[6,41–44]. Errors in precortical areas of visual processing (the retina, optic nerve, thalamus) cause subsequent errors in higher cognitive processes. The decrease in the information flow in precortical visual pathways probably leads to a distorted condition where the brain evaluates and models a situation based on incomplete or incorrect input signals and is not able to properly modulate and integrate them into consciousness[5,45,46]. A low signal-to-noise ratio[47] in particular results in an increased level of vagueness related to the nature of a percept/signal, leading to a disruption of the decision-making process[48]. This leads to compensation effects in the form of overlapping receptive fields of retinal cells, inhibition of visual information

---

[1]Third Faculty of Medicine, Charles University, Prague, Czech Republic. [2]Present address: Center for Advanced Studies of Brain and Consciousness, National Institute of Mental Health, Klecany, Czech Republic. ✉email: petr.adamek@nudz.cz

preprocessing caused by a higher number of errors, and excessive amplification of sensoric and noise signals[49]. This pathological process may also be facilitated by dopamine (DA)[50], acetylcholine (ACh)[51], and glutamate[52] dysregulation modifying the electro-physiological response to stimuli.

Top-down modulation of visual perception is provided via several complementary mechanisms and, given the fact that the quality of visual perception affects higher cognitive functions, impairments in all of the modulatory mechanisms may give rise to various cognitive schizophrenia symptoms apparent in tasks challenging attention, working memory, or associative and executive functions. Attention and working memory are a basis for higher cognitive functions, such as associative and executive functions, and, vice versa, executive functions control attention and working memory in a feedback loop[53–55].

Top-down control, as well as bottom-up processing of visual perception, may be disturbed by alterations in cortical and subcortical brain regions as documented in schizophrenia patients and also supported by animal models. In postmortem and brain imaging studies of schizophrenia patients, abnormalities including enlarged lateral ventricles and reductions in gray and white matter in subcortical and cortical regions were observed[56–58]. In rodent animal models, schizophrenia-like symptoms after lesions in the prefrontal cortex (PFC), ventral hippocampus (homological to the anterior hippocampus in humans), amygdala, or nucleus accumbens have been documented. Interestingly, these lesions resulted in altered connectivity or neurochemistry of the limbic circuit or modifications to the cytoarchitecture of the PFC[59–63]. Together, the aberrant early stages of visual processing represent the candidate mechanism for explaining the development of core schizophrenia symptoms.

The aims of this article are to: (1) summarize the current knowledge of visual perception impairment in schizophrenia patients on each level of the precortical visual signal processing pathway (the retina, optic nerve, LGN) and the effect of such impairments on visual perception, (2) compare pathophysiological alterations of the visual precortical pathway with cortical pathological changes documented in schizophrenia patients, and (3) propose a new context of schizophrenia symptoms stemming from the pathophysiology of the visual signal processing.

RETINA

Information about the external environment enters the visual system through the retina, where the early phases of input signal processing and transformation take place. The input signal is modulated by more than twenty types of ganglion cells responsible for converting visual information into an electro-chemical signal, the characteristics of which correspond to various attributes of a visual percept[64].

Abnormalities in retinal electrophysiological responses to stimulation by light[65], morphological alteration of retinal structure[66], and alterations of retinal metabolic processes[67] may be found in schizophrenia patients. Although visual perception is one of the most intensively studied and well-understood fields of neuroscience, reports on the topic of retinal structure and function comprise only 2% of all studies of visual perception in schizophrenia[49]. At the same time, it is a malfunction of the retina that most often leads to lower sensitivity to contrast and to high spatial frequencies of an image stimulus[68–70], distortion of color perception, reading issues[71,72], and some types of visual distortion and hallucinations[73–75] in schizophrenia patients. However, visual hallucinations, in particular, are a relatively rare symptom of schizophrenia and only occasionally appear alone; they are more often accompanied by hallucinations of other modalities[76]. This fact may suggest a common pathophysiological mechanism underlying hallucinations of visual and other perceptual domains. In comparison with only unimodal hallucinations, a combination of visual and auditory hallucinations is associated with an increased severity of gray matter volume (GMV) reduction. The reduction in GMV in first-episode patients with combined visual and auditory hallucinations is especially prominent in the occipital cortex and frontoparietal areas[77,78]. Interestingly, the severity of GMV reduction in certain areas is accompanied by increased functional connectivity and is related to the severity of both visual and auditory hallucinations. The mechanisms linking hallucinations and GMV reduction are yet to be discovered[77–79]. Congruently, the expression of auditory hallucinations alone is also related to more severe impairments already present in the retina[78]. Together, studies focused on the interconnection between visual pathological phenomena (such as visual hallucinations and illusions) and their relationship to abnormalities in other perceptual modalities may, therefore, help to reveal the basic mechanism related to schizophrenia development in general.

Morphological and pathophysiological changes in the retina

In vivo studies using ocular coherence tomography (OCT) have confirmed changes in the retinal structure. The majority of studies have focused on the atrophy of retinal nerve fibers (RNFL) representing a decline in ganglion cell axons and the overall thinning of the macula[80]. Thinning of the inner plexiform layer and the inner nuclear layer (Fig. 1) in schizophrenia has also been reported[81]. Interestingly, thinning of the retina in the foveal, nasal, parafoveal, and temporal-parafoveal regions of the macula as well as a reduction in the outer nuclear and inner plexiform layers (Fig. 1) have been related to negative symptom severity (a negative score on the Positive and Negative Syndrome Scale negative subscale) and selective deficit to LSF contrast sensitivity[70]. In addition, the loss of ganglion cells in the temporal parafoveal region of the retina was associated with magnocellular ganglion cell loss throughout the disease progression[70].

The currently open question is whether structural and functional alterations to the retina occur due to trans-synaptic retrograde degeneration originating from the regional pathology at the higher steps of visual pathway or vice versa.

Recent studies have shown that in the early stages of schizophrenia, there was a loss of GMV in the thalamus[56]. As the schizophrenia progresses, GMV loss expanded to the frontal lobes and then to the temporal lobes, occipital cortex, and cerebellum[58,82]. These studies thus suggest a retrograde nature to the retinal ganglion cell (RGC) volume loss process. When the thalamic volume decreases, it causes a loss of connectivity for RGC axons and thus their subsequent inflammation. OCT studies have shown that atrophy of ganglion cell axons and thinning of the macula manifest mostly during the chronic and long-term chronic phases of schizophrenia[83,84], which would also indicate that a retrograde origin for retinal cell degeneration is more likely than an anterograde origin is.

Without further studies, however, we cannot rule out an anterograde nature to the process, which can be started by dysregulation of DA[66,80] and glutamate transmission[85]. In pathological cases, both of these transmitters are capable of causing retinal atrophy and a loss of axons in specific retinal layers. This loss is thought to be caused by over-stimulation of the N-methyl-D-aspartate receptor (NMDAr). This results in an increase in the intracellular Ca^{2+} concentration in RGCs, resulting in excitotoxic damage as seen in other compartments of the central nervous system (CNS)[86,87]. Congruently, activation of GABA interneurons by nitric oxide has been proposed as a preventive mechanism of excitotoxic degeneration and a mutation of nitric oxide synthase was identified as one of the genetic risk factors of schizophrenia[88].

Thinning of the retinal layers may also be related to abnormalities in blood supply. Recent studies using OCT
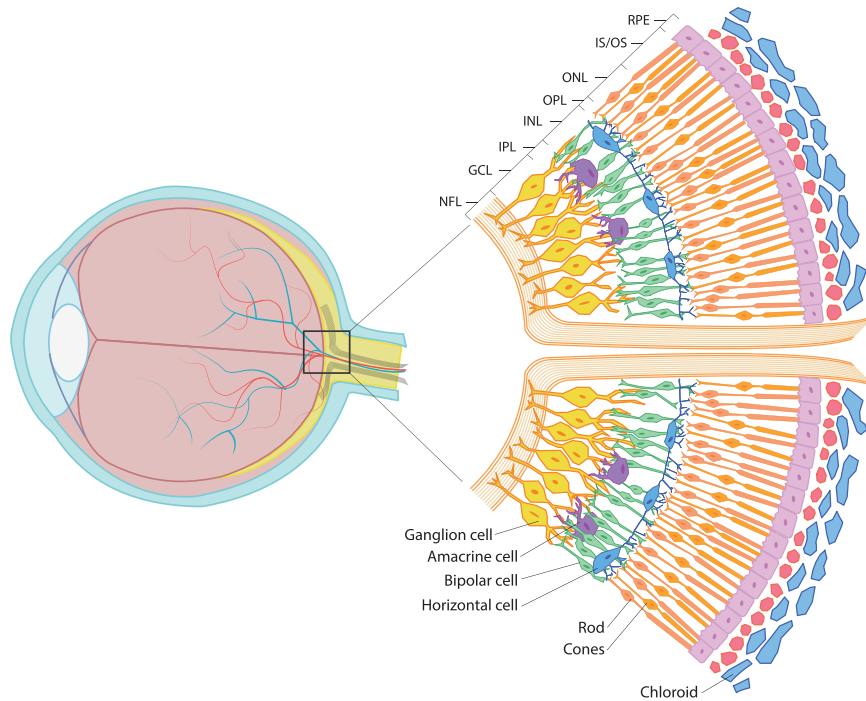
Fig. 1 Retinal layers. The composition of the individual layers of the retina in the area of the optic nerve. NFL nerve fiber layer, GCL ganglion cell layer, IPL inner plexiform layer, INL inner nuclear layer, OPL outer plexiform layer, ONL outer nuclear layer, ELM external limiting membrane, IS/OS rod and cone inner and outer segments, RPS retinal pigment epithelium. Redrawn from retinareference.com.
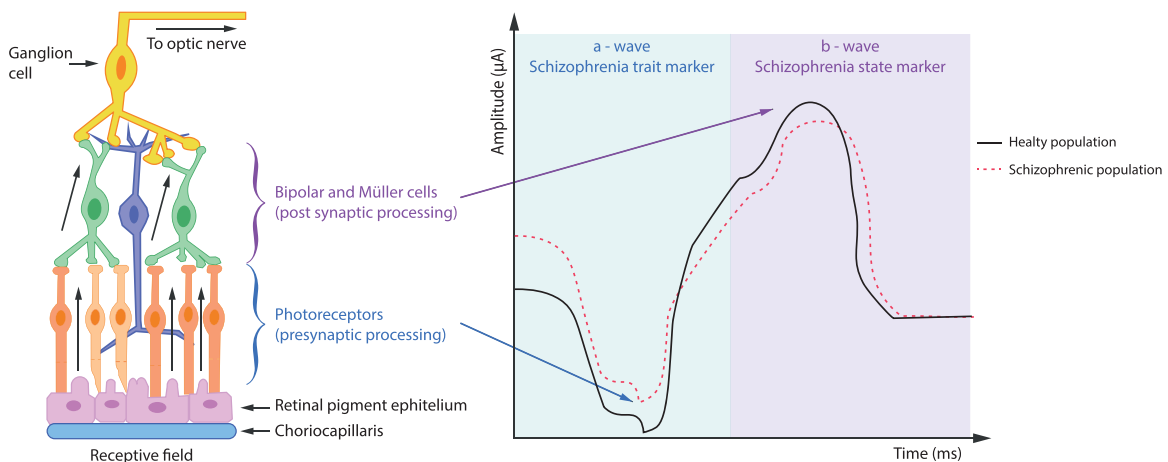

Fig. 2 Schema of ERG signal from retinal cells. An illustration of the retina (left) and a representative ERG comparing HCs and schizophrenia patients (right). In the dark-adapted retina, a light stimulus elicits a presynaptic response from photoreceptor cells, represented by the downward-deflecting a-wave. The subsequent postsynaptic response, mediated largely by bipolar and Müller cells, produces the b-wave. The a-wave amplitude (measured from the baseline to the trough of the a-wave) depends on the intensity of the light stimulus and the integrity of the photoreceptors. The b-wave amplitude (measured from the trough of the a-wave to the peak of the b-wave) depends on the a-wave and the integrity of signal transmission within the retina. Redrawn from Hanjin Deivasse web illustration.

angiography have demonstrated changes in retinal microvasculature in terms of both reduced perfusion and vessel density. These abnormalities are mainly associated with RNFL thinning (see above)[89]. Previous studies also observed changes in retinal venules, which dilate mainly due to chronic retinal hypoxia[90–92]. However, a similar effect on small vein widening was also observed as a result of an increased concentration of retinal DA[93].

If we were able to understand the retrograde or anterograde origin of the onset of morphological changes, it would be possible to target therapy specifically to these sites, thereby slowing or stopping the degradation of individual cell populations of the retina, LGN, and optic nerve.

Changes in the electrophysiology of retinal cells

Morphological and biochemical changes in the retina of schizophrenia patients are accompanied by alteration in the electrophysiological response of individual retinal cells to light stimulation. Abnormalities in sensitivity to certain wavelengths, frequencies, and intensities of light during stimulation were recorded by electroretinography (ERG)[65]. These abnormalities manifest as changes in amplitude and a delayed onset of the electrophysiological response to a light stimulus (latency), but also in the structure of the a- and b-waves (Fig. 2)[94]. The largest ERG study of psychiatric disorders performed to-date (150 schizophrenia patients, 150 patients with bipolar disorder, and 200 healthy

control subjects [HCs]) showed a reduction in amplitude of the a-wave and a later onset of the b-wave during stimulation focused on the electrophysiological response of cone cells in both patient groups[95]. In contrast, a reduction in b-wave amplitude, which was produced by a simultaneous response by Müller glia, responsible for the capture of neurotransmitters from intercellular space and the regulation of potassium concentration, and bipolar cells, which provide the connection between the inner and outer plexiform layer in the retina, was observed only in the schizophrenia patients. A decrease in the amplitudes of the a- and b-waves during stimulation aimed at the combined electrophysiological response of both rods and cones was also found in both patient groups. The study authors presumed that aberrations in the b-wave latency and amplitude may be considered an early and very specific biomarker of schizophrenia. Conversely, a decrease in the a-wave amplitude may plausibly be connected only to the acute phase of the disorder, as after an eight-week treatment no significant differences were observed between the schizophrenia patients and HCs[96].

Biochemistry of the retina

Changes in the pathophysiology of the retina in the schizophrenia population are accompanied by biochemical changes, which stem from an imbalance in excitatory and inhibitory neurotransmission, as outlined above. One of the most important catecholaminergic neuromodulators reaching the highest local concentration within the primary visual system in the retina is DA[73,86]. DA is one of the main neuromodulators in the mammalian brain and is considered, within the scope of the theoretical model of schizophrenia, one of the principal mediators of positive symptoms via the dopaminergic mesolimbic pathway, as well as negative symptoms via the mesocortical pathway[97]. Moreover, dopaminergic substances such as cocaine and amphetamine induce or trigger psychosis[86]. The concentration of retinal DA is not constant and is affected by various factors such as circadian rhythms and age[98]. Animal studies have confirmed that the concentration of retinal DA is regulated via stimulation of the hypothalamus, followed by activation of retinopetal neurons, which release histamine. The axons of these neurons run through the optic nerve to the boundary of the inner plexiform and nuclear layers. Here, the release rate of intercellular histamine, which binds itself to the D_1R receptors of DA-releasing amacrine cells, may be increased[99,100]. However, there is only indirect evidence of this mechanism in humans. Recent methods only enable modulation, the ERG curve of the b-wave via positive stimulation through food (hypothalamus activation) or by administering the DA agonist methylphenidate[101].

The majority of dopaminergic cells are located between the inner nuclear and plexiform layers of the retina[102]. They respond to DA through the metabotropic G_s D_1 receptors located at the membrane of bipolar, horizontal, amacrine, and ganglion cells[103] and via metabotropic G_i D_2 receptors at the membranes of both rods and cones (Fig. 3). D_2 receptors are also present at DA-releasing AII amacrine cells. D_2 on these cells function as autoreceptors regulating the release of DA[104–106].

Extracellular DA modulates the degree of excitability of retinal cells directly and indirectly. The direct connection functions via synaptic or volume transmission and bonding to D_1 and D_2 receptors. DA indirectly affects retinal cells in multiple ways: (1) It alters the probability of opening/closing membrane ion channels, but also the length and frequency of the opening/closing[107]. (2) It regulates the excitability of the horizontal intercellular gap junction in the inner plexiform layer, where a decrease in the DA concentration increases the permeability of the gap junction in AII amacrine cells. Their activity modulates the excitability of metabotropic ON-center bipolar cells (BCs)[108] (Fig. 3). Excited AII amacrine cells have an inhibitive effect on ionotropic OFF-center
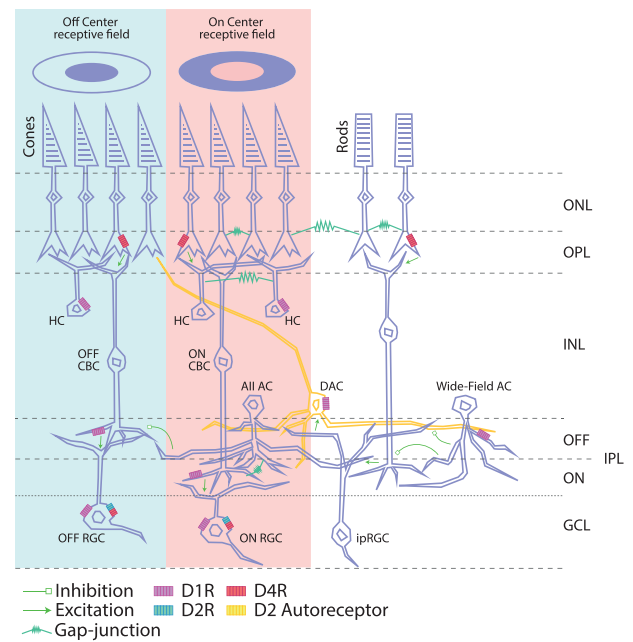

Fig. 3 Distribution of DA receptors in retinal cells. Schematic of the retinal circuitry with cell types expressing specific DA receptors in the retina. The DA receptors D_1R, D_2R, and D_4R and D_2 autoreceptors localized on various cell types are indicated in purple, green, yellow, and red. The dopaminergic amacrine cells (DACs; orange) stratify primarily in the outermost layers of the IPL and send axon-like dendritic projections to cone terminals in the OPL and to the inner layers of the IPL, where they contact AII amacrine cells (ACs). Synaptic excitation and inhibition are illustrated by arrows and bar-line (green). Gap-junctions are shown as sawtooth symbols. The two concentric circles at the top represent OFF-center and ON-center RGCs, which respond oppositely to light in the center and surroundings of their receptive fields. DAC: aopaminergic amacrine cell, HC horizontal cell, RBC rod bipolar cell, CBC cone bipolar cell, AC amacrine cell, RGC retinal ganglion cell, ipRGC intrinsically photosensitive RGC. Redrawn from Roy & Field[50].

BCs (Fig. 3) and, therefore, suppress distortion and noise at the frequencies and intensities of action potentials, which are transferred to ganglion cells[109]. Conversely, increased DA concentrations inhibit horizontal communication and the permeability of gap junctions in AII amacrine cells, while also altering the continuity of action potential changes in ON-center BCs[106,110,111]. This increases their sensitivity to local stimulation of a particular group of photoreceptors and inhibits peripheral stimulation. Fluctuations in extracellular DA concentrations also remodulate the nature of the signal exiting the RGCs and BCs and, therefore, affect the signal from ON- and OFF-centers of receptive fields[112]. Long-term pathological changes in DA concentrations may lead to a loss of spatial vision and temporal sensitivity[73]. (3) DA modulates the response of retinal GABAc receptors, which participate in the communication between retinal cones and bipolar and horizontal cells—in other words, they modulate the intensity of the signal output from photoreceptive cells via the degree of membrane hyperpolarization, which regulates its excitability[113].

Glutamate is the main excitatory neurotransmitter in the retina and the only output neurotransmitter of all photoreceptors[114]. Glutamate is released by photoreceptors during depolarization (the phase when photoreceptors are not stimulated by light) and an increase in its concentration affects ionotropic OFF-center BCs. Conversely, stimulation of photoreceptors by light is followed by hyperpolarization, the concentration of glutamate decreases, and metabotropic ON-center BCs are stimulated. The glutamatergic system is generally related to positive, negative[70], and cognitive symptoms of schizophrenia[83] via hypofunction of NMDAr.

Dysregulation of NMDA also leads to an increased release of DA[115], which affects the extent of positive symptoms such as visual distortions, hallucinations, and altered performance in psychophysiological testing of visual perception[116,117]. Changes in visual perception are also connected to excitotoxic damage to photoreceptive cells and disrupt the perception of motion and high spatial frequencies of image stimuli[70,87]. Animal testing on rodents has shown that it is possible to reduce the ERG b-wave amplitude of Müller cells during artificially induced reduction of glutamate transmission via the glutamate aspartate transporter[118].

The visual perception processes described above may be studied by administering agonists or antagonists of specific receptors. However, it is difficult to say if an observed effect occurs on the retina or downstream in the cascade of visual perception processes. Administering D_2 antagonists (haloperidol, benzhexol, and fluspirilene) to schizophrenia patients for three weeks caused a decrease in sensitivity to contrast of visual stimulus compared with HCs. However, sensitivity was not decreased globally and depended on the stimulus orientation on the vertical or horizontal plane of the visual field[73,119]. Antipsychotics (trifluoperazine, fluphenazine, and haloperidol) also inhibited sensitivity to high and medium spatial frequencies of image stimuli. Conversely, the opposite effect was observed for LSFs[68]. In both cases, the physical saliency was affected. A general increase in sensitivity to contrast after dopaminergic stimulation via L-dopa was observed in both schizophrenia patients[120] and HCs[121]. A hyperdopaminergic state during early phases of schizophrenia is responsible for increased sensitivity to LSFs and related excessive excitation of ganglion cells, which constitute magnocellular pathways responsible for conducting a signal to the visual cortex[122]. It is plausible that all of the aforementioned effects are associated with the ability of DA to affect the size and sensitivity of retinal receptive fields for distinct spatial frequencies[123] via inhibition of the gap junction of retinal horizontal cells and reduction of the amplitude induced by light incident on the photoreceptors. Both of these effects would then have a physiological basis in dopaminergic mechanisms related to brightness adaptation[73].

It is important to emphasize that the retina is considered a part of the CNS, as during embryonic development it originates from the same tissue as the brain and shares with it many biological processes, including the role of neurotransmitters and their receptors, lateral connectivity, and feedback mechanisms[124]. Therefore, changes in retinal function may be caused by schizophrenia itself, its course, and antipsychotic medication[124,125]. Some of the observed retinal dysfunctions may be related to other factors and comorbidities, such as systemic diseases (diabetes, hypertension), smoking, antipsychotic medication, drug abuse, sex, obesity, attention span, degree of arousal, and motivation, as they influence the retina via histaminergic and serotonergic inputs from brain regions[49].

The pathology of retinal function may be generally characterized in two basic categories: (1) hypofunction caused by damaged retinal cells due to glutamate dysregulation, and (2) hyperfunction due to excessively high DA concentration. However, both of these effects cause a modulation of optosensoric signals, which are transferred further to higher levels of precortical and cortical visual processing circuits.

Optic nerve and LGN

A small proportion of the optic fibers are diverted from the retina into the retinohypothalamic tract, which leads to the anterior hypothalamic nucleus. This connection affects pupilar dilation (sympathicus) and constriction (parasympathicus)[126]. However, up to 90% of the signal is passed through ganglion cell axons, forming three independent pathways (magno-, parvo-, and koniocellular) inside the optic nerve, into the optic chiasm, where some of the nerve fibers cross, and further into the LGN of the thalamus[127]. According to recent findings, the regulation, timing/distribution, and strength of signal input from the retina into specific parts of the primary visual cortex (V1) occur within the LGN[128]. However, regulation of the output signal from the LGN is a very complex process regulated by several feedforward control mechanisms. The most prominent non-retinal inputs, which also react to the output signal from the LGN, are glutamatergic inputs from the cell of the VI layer of the V1 operating on both the ionotropic and metabotropic glutamate receptor pathways and directly affecting the depolarization of relay cell (RC) membranes in the LGN. In principle, the LGN consists of two cell classes. First, the glutamatergic RCs, which send axons to the visual cortex, and second the interneurons (INs), the axons of which remain in the LGN (Fig. 4a). The visual signal in the LGN is regulated by local inhibitory neurons and thalamic reticular nucleus (TRN) inhibitory neurons. These neurons are connected by feedforward and feedback circuits (Fig. 4a). The feedforward pathway consists of the classic triad synapse[129]. The afferent axons of the optic nerve connect to the dendrites of LGN INs and RCs. The INs and RCs then form a dendro-dendritic connection at the same synapse. In the
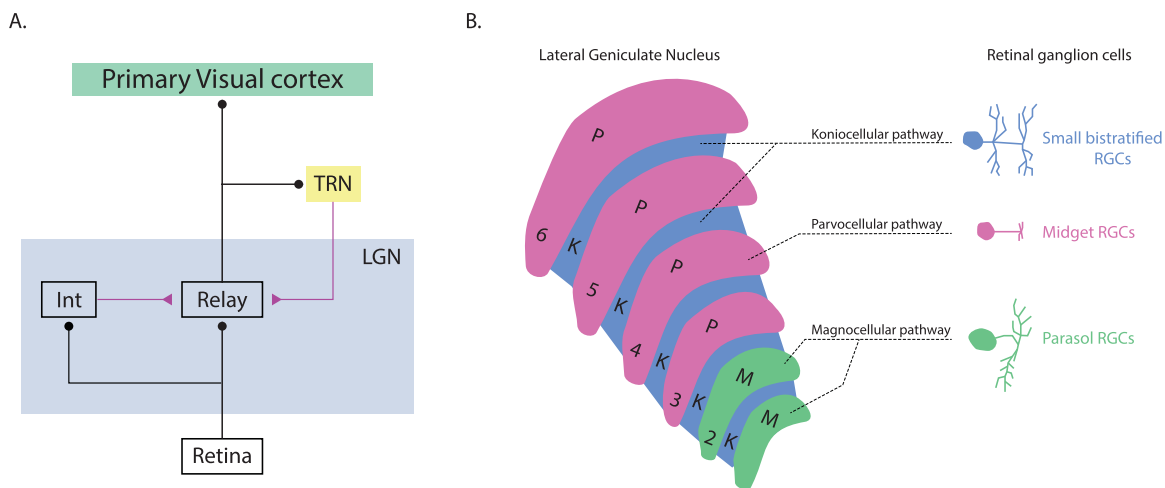

Fig. 4 **Structure of the LGN with three distinct layers.** Simplified diagram of visual thalamic circuitry and the LGN. **A** Diagram of feedforward and feedback inhibitory pathways that influence LGN RCs. Excitatory inputs are indicated in purple. Inhibitory inputs are indicated in black. TRN: thalamic reticular nucleus; LGN lateral geniculate nucleus; Int LGN interneuron. Modified from Casagrande & Xu[129]. **B** LGN diagram with ganglion cells type. RGCs retinal ganglion cells. Redrawn from Kim et al.[141].

Table 1. Morphological and functional characteristics of the visual pathway.

Characteristic	Magnocellular	Parvocellular	Koniocellular
Ultimate destination in the brain	Predominantly parietal lobe	Predominantly temporal lobe	Probably the V1
Sensitivity to movement and flicker	Very sensitive	Insensitive	Not sufficiently described
Spatial frequency summation	Non-linear	Linear	Linear
Ability to resolve details	Good at resolving coarse detail	Good at resolving fine detail	Overlap of M and P cells
Ability to detect contrast	Sensitive to low contrast objects	Sensitive to high contrast objects	Overlap of M and P cells
Effect of blur	Relatively insensitive to blur	Greatly affected by blur	Not sufficiently described
Area of visual field where most sensitive	Peripheral vision/ large	Central vision/ small	Not sufficiently described
Ability to discriminate colors	Color insensitive	Color sensitive	Yellow and violet-blue sensitive
Spatial frequency	Low	High	Overlap of M and P cells
Temporal frequency	High	Low	Overlap of M and P cells
Response latency	Short	Long	Medium
Temporal resolution	Fast	Slow	Medium
Dendritic field size (µm)	30–300 µm	10–100 µm	Not sufficiently described

case of feedback, the TRN inhibitory neuron receives a signal from the axon of the RC. The TRN neuron sends an inhibitory connection back to terminate on the dendrite of the same RC (Fig. 4). Both of these inhibitory circuits also contribute to the character of the signal that is going through the RCs[128,130].

Further modulation of the output signal comes from cholinergic endings innervating the INs and RCs of the LGN[131]. The contribution of cholinergic transmission to the overall nature of the signal emanating from the LGN is considerably complicated. This is because of the presence of slow metabotropic (M1) and fast ionotropic muscarinic ACh receptors in the membranes of RCs (in both cases, their activation leads to depolarization)[132]. Additional ACh M2 receptors are present in INs and TRN cells and their activity leads to hyperpolarization. Overall, however, we can say that ACh inputs to the LGN have an excitatory effect. RCs are depolarized and inhibitory feedforward and feedback circuits are blocked[128].

In the case of DA, the density of dopaminergic innervation is lower in the LGN compared to the rest of the thalamus[133]. Animal studies have demonstrated the presence of D_1 and D_2 receptors in the membranes of LGN RCs. Stimulation of D_1 receptors led to inhibition of their excitability. Conversely, activation of D_2 receptors had an excitant effect on their glutamatergic synapses[134] and, therefore, the overall sensitivity to local contrasts within the framework of visual perception was increased[128,135–137].

Like the retina and other parts of the visual system, the LGN shows the presence of receptive fields responding to specific aspects of the visual scene[138]. Recent studies have shown possible modulations of receptive fields based on feedback from the V1[139]. However, a key outstanding question, particularly for understanding visual impairment in schizophrenia, concerns the influence of monoamines and ACh on this modulation.

Magnocellular, parvocellular, and koniocellular pathways
The morphological structure of the LGN is characteristically constituted of visible distinctive layers, which reflect the structure of the optic pathway. These layers are composed of three separate nervous pathways, which are divided into twelve layers (four dorsal parvocellular [PC], two ventral magnocellular [MC], and six koniocellular [KC] interlayers; Fig. 4). The individual retinal input pathways differ not only in the sensitivity of their cells to the spatial frequencies of an image, electromagnetic spectrum wavelengths, and contrast, but also their own physical morphology[140].

The majority of the MC pathway consists of axons of parasol RGCs[141]. The primate retina is composed of two types of parasol

puncta: ON-parasol cells depolarizing when light strikes the center of their receptive field and OFF-parasol cells with the opposite reaction[142]. These cells have a larger dendritic field (30–300 µm) compared to midget RGCs and their input signal is ca. 80% composed of amacrine cell activity with BCs contributing the remainder of the signal. MC pathways react to the velocity and direction of a moving object—its spatial localization. They are sensitive to low contrasts and LSFs. On the other hand, they have high temporal resolution. The proportion of the input signal from rods and cones to the MC pathways depends largely on the light conditions[143] (Table 1). They assist in stereopsis, depth perception, hyperacuity, and recognition of objects in a visual scene, including associations between them and separating individual objects from the background[141,144]. They play a central role in the perception of the overall organization of the stimulus[145]. MC pathways are highly myelinated and signal transmission to the visual cortex is considerably faster compared to the two other pathways. These pathways also play a key role in directing eye movements and in the coordination between our body and moving objects[139].

The signal passing through MC pathways is further processed and continues into specific areas of the V1. However, some recent studies have questioned the continuation of magnocellular pathways into the dorsal stream, based on the coactivation of ventral stream regions by low spatial frequencies in some specific visual tasks[146,147].

PC pathways are predominantly composed of midget RGCs. These cells have small bodies and their dendritic branching is only about 5–10 µm in diameter in the central part of the retina (it can reach up to 225 µm in the peripheral regions)[141,148]. This corresponds to smaller receptive fields. Midget cells are mainly localized in the central part of the retina and form a one-to-one connectivity with the midget BCs that receive the signal from the single cone[149]. As with parasol RGCs, midget RGCs have ON- and OFF-center types. PC pathways are sensitive to colors, high spatial frequencies, shape, and other details of objects in a visual scene (Table 1). Their speed of transferring nerve impulses and degree of myelinization are lower. The summation of their membrane potentials is linear with a low action potential velocity (Table 1). They are also able to react during the entire effect duration of a stimulus. PC pathways end mainly in the lower parts of the IVC layer V1 (IVCβ and IVCctr). A smaller proportion of their endings are also located in the IVA layer (Fig. 5).

KC pathways are predominantly composed of axons of small bistratified RGCs[150]. These cells are assumed to have a supportive function for color vision with low spatial resolution[141]. Animal studies performed on primates showed the reaction of some KC cell groups within the LGN to chromatic stimuli, violet-blue
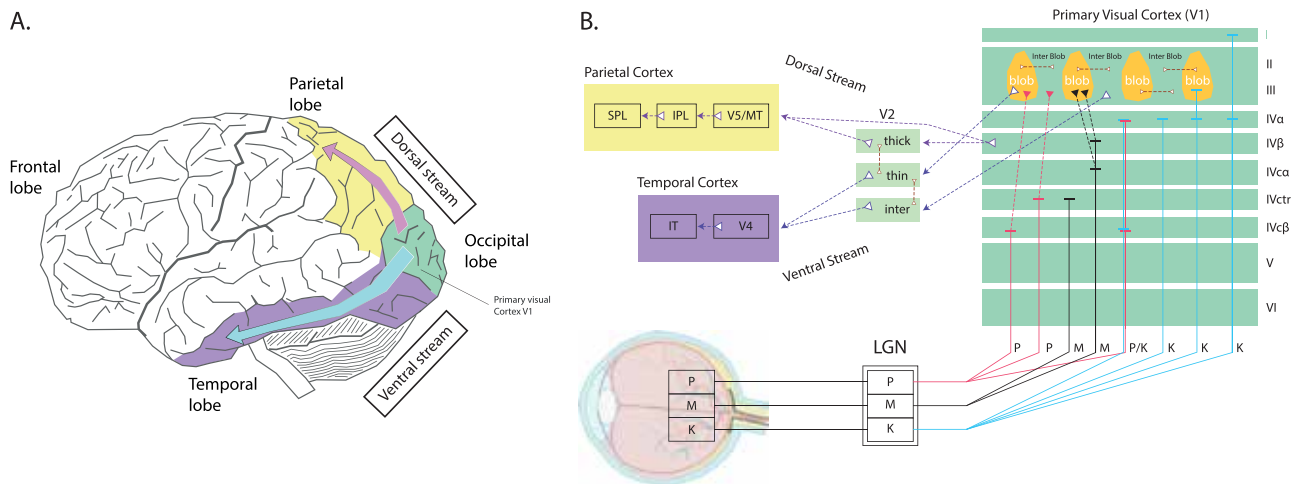
Fig. 5 Visual pathways and brain streams. A The ventral (purple) and dorsal (yellow) streams of visual information processing. **B** A detailed scheme of signal distribution from PC, MC, and KC visual pathways to the LGN and further to the primary (V1) and secondary (V2) visual cortex and subsequently to the dorsal or ventral stream. Redrawn from Casagrande & Xu[129].

(400–470 nm) and yellow (600 nm) wavelengths, and brightness[151–153]. KC pathways end in cytochrome oxidase blobs contained in the I, III, and IVα V1 layers. Some parts of these blobs are also present in the structure of the VI layer of the V1. However, the exact function of the KC interlayers in humans is not yet fully understood[154].

It is useful to recall that the size of the receptive field plays an important role in sensitivity to specific frequencies of image perception[155,156]. This sensitivity is to some extent determined by the specific morphology of each class of RGCs, specifically by the size of their dendritic field. In normal physiological conditions, receptive fields are fine-tuned by DA, which allows adaptation to the specific light conditions of the surrounding world[106,157]. Future research should answer the question of how much DA and retinal morphological changes in schizophrenia patients alters the sensitivity of the human receptive field and how these changes affect the spatial integration of visual perception in higher precortical and cortical areas.

CORTICAL INTEGRATION AND PROCESSING OF VISUAL STIMULI

Earlier studies pointed to the central role of MC pathways in the disruption of visual perception in the schizophrenia population, predominantly based on reduced contrast sensitivity at LSFs[6,8,13,45]. This approach was later criticized for several reasons[32], in particular, the uncertainty that the stimuli used in the studies really activated only the MC pathways. Another point was the lack of distinction between the subcortical MC pathway and the cortical dorsal stream (Fig. 5)[26,146]. Thus, the overall disruption of visual stimulus integration in the cortical areas is currently attributed to gain control mechanisms[112]. The latter at the molecular level is related to the ability of signal integration on pyramidal neurons and its modulation within the feedback and feedforward circuit. The core modulator in this case is thought to be DA[31]. DA at the cell body increased the influence of bottom-up inputs through a combination of augmenting a slow, depolarizing influence (Na+) and decreasing a slow, hyperpolarizing current (K+)[31,158].

In general, visual processing consists of a set of mechanisms optimizing perception of visual information further utilized in goal-directed behavior. The quality of the perceived information is controlled from both directions, ascendently (bottom-up) and descendently (top-down). Throughout visual processing, the gain of information is controlled precisely and the information

from the lower levels of the visual system is integrated on every level of processing[6]. Precortical processing is performed during the course of projection from the retina to the V1 and in subcortical circuitries participating in higher cortical processing. Subcortical structures cooperating on higher processing include higher order thalamic nuclei (pulvinar, mediodorsal), the basal ganglia, and the amygdala. Higher order thalamic nuclei participate in the integration of cortical information and the reconnection of distinct cortical compartments or working memory[159,160]; the basal ganglia contribute to filtration of information, working memory, and attention[161]; and the amygdala cooperates on information contextual analysis or shifting visual attention towards emotional stimuli[162]. In addition, the thalamic function is strongly influenced by monoamines and ACh[128]. These neuromodulators amplify the bottom-up and top-down signal-to-noise ratio[163].

Top-down control is assumed to be initiated by approximate information about an object carried rapidly via MC pathways to the visual cortex and through the dorsal stream to the PFC. Complementary to that, the PC pathway carries more detailed information about visual stimuli in a slower manner to complete and specify the image[164,165]. The two pathways cooperate and coordinate with each other[166]. The theory of a direct pathway from early visual areas to the PFC corresponds to immediate reactivity of PFC areas to visual stimuli. Together with early visual areas, the caudal middle frontal cortex was activated. This cortex includes the frontal eye field (FEF), orbitofrontal cortex (OFC), and ventromedial PFC[167]. Some studies have proposed a direct connection of the MC pathway to the lateral PFC[164]. As the brain structure responsible for executive functions, planning, and making decisions, the PFC analyzes the inner and outer contexts of information and provides top-down control over other brain areas and neural networks and their synchronization[168]. The FEF controls saccades and was shown to have a direct projection to the V4[169,170]. The OFC and ventromedial PFC connect with the amygdala and process emotional stimuli. The FEF, OFC, lateral PFC, and ventromedial PFC all have connections to the inferior temporal cortex (IT), a key area for integration, semantic memory, and recognition[171]. The PFC is assumed to project the information received from the MC pathway to the IT, which afterwards categorizes the approximate information and projects the integrated information back to the occipital cortex to sharpen the attention and acquire the most relevant information about the object of observation. fMRI studies focusing on the perception of visual illusions have shown impaired top-down processing (in the
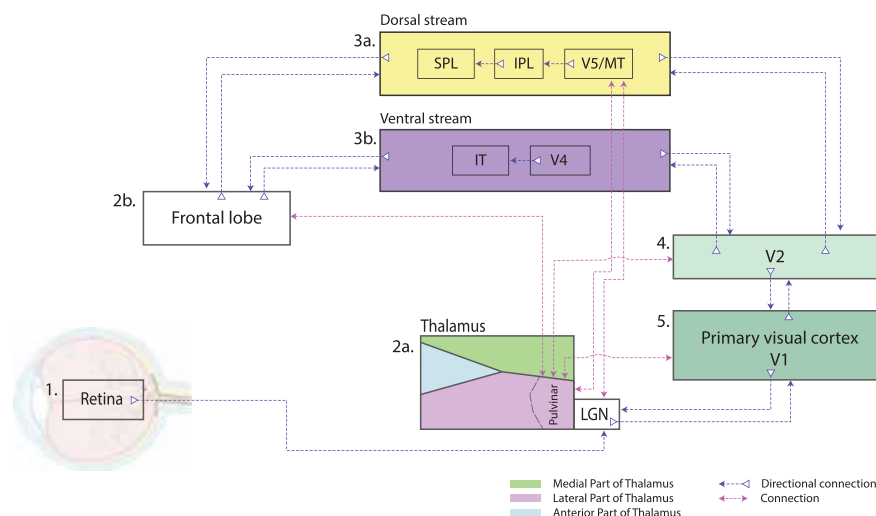
Fig. 6 Aberrant signal propagation and subsequent physiological changes. This simplified scheme illustrates the hypothesis of the early spread of an aberrant signal within the visual circuit and the physiological changes associated with it. **1** In the early stages of the disease, an aberrant signal is formed on the retina and further propagates within the precortical and cortical visual circuit. **2a/b** The first areas that are likely to fail to adapt to the unstable signal and where there is GMV thinning are the thalamus and areas of the frontal lobe. **3a/b** From there, the pathophysiological changes spread into the lower visual processing areas (**4** and **5**). SPL superior parietal lobule, IPL inferior parietal lobule, V5/MT middle temporal visual area, IT inferior temporal cortex, V4 visual area 4, V2 secondary visual cortex, LGN lateral geniculate nucleus.

frontoparietal network) in patients with schizophrenia and a predominant emphasis on the integration of bottom-up sensory stimuli[26,38,172].

The process of integrating visual information consists of excitatory and inhibitory projections, when the purpose is usually to enhance perception about the object of interest while simultaneously suppressing perception of the surroundings. Nonetheless, the surroundings can have a major impact on the accuracy of object identification[173]. Higher processing of visual information includes executive functions, in which we see impairment in schizophrenia patients, such as working memory[174], long-term memory and learning[175], object[176] or facial recognition[177], and context integration[26].

Abnormalities in higher cognitive processing lead to the creation of an abnormal perception of surrounding reality, which in turn supports abnormal perception in a positive feedback loop. Imbalance in bottom-up and top-down visual processing affects selective attention, visual working memory, object and facial recognition, and memorization of visual information[164,178,179]. In schizophrenia, imbalances in bottom-up and top-down processing create conditions for symptoms consisting of visual distortions, alternated perceptions of illusions, visual hallucinations, and cognitive impairments including social cognition[180,181]. It is possible to start considering the connection between perceptual disorders and cognitive dysfunctions or specifically to consider cognitive dysfunction as a consequence of long-term imbalances in the signal-to-noise ratio of sensory modalities of visual perception.

Instability of the inner world model as a schizophrenia trigger
Visual perception, the dominant source of information in the development of our inner world model, modulates our experience of reality. The disruption of visual perception modalities in schizophrenia may contribute to the development of an incorrect model of reality[182], which further accelerates the development of the disease itself.

As mentioned above, schizophrenia is characterized by instability in the input visual signal, with hypersensitivity to LSF in the early stages of the disease (before and during the first episode). It is followed by a progression to hyposensitivity and

affects other frequencies in the visual field. The instability of the input signal (bottom-up) then leads to biased prediction models; more precisely, the unstable signal-to-noise ratio does not allow the creation of a stable/dominant model that would adjust intrinsic reality predictions and contextual modulation.

The most probably scenario is as follows: The long unstable and noisy signal from the visual periphery is transmitted to other areas within the precortical circuit. These areas modify the primary noisy signal and abstract the outputs for higher cortical areas. In cortical pyramidal neurons (PNs), further contextual modulation/abstraction of the signal occurs[31] in terms of suppression, amplification, or synchronization[26]. Higher cortical areas, led by the PFC[183], make predictions based on this signal[183]. However, the formation of long-term stable predictions is suppressed by variable and unstable noise from lower areas of the perceptual cascade. We speculate that the demanding process of adaptation to this noise signal in higher cortical areas may in the long run lead to a neurotoxic process connected to reduced connectivity among PNs, preventing the formation of stable representations. Gray matter reduction, which is strongly associated with schizophrenia, is attributed to an overall reduction in the number of synapses on the PNs[184]. These changes may then propagate back to lower stages in the perceptual cascade, adding new noise to the already noisy signal. This time, however, due to the reduced synaptic connectivity (Fig. 6).

The loss of neural connections in the PFC is also influenced by genetic factors such as gene expression in inhibitory GABAergic INs. Suppression of GABAmergic INs leads to a decrease in gamma synchrony affecting synapse formation and stability[184,185]. Thus, in schizophrenia patients, reduced connectivity in the cortex could be compounded by the addition of an unstable signal from the periphery that forces a new network modulation based on its instability.

Based on these considerations, we hypothesize that increased noise in the signal from the sensory periphery may serve as a trigger mechanism for the development of schizophrenia. This assumption is indirectly supported by the probable protective effect of congenital blindness or early cortical blindness in the high-risk population[186,187], even after taking the low incidence of these health conditions in the general population into consideration[46,186–188]. There are no known schizophrenia cases in people who have

suffered congenital blindness or lost vision at a very early age. Traditionally, there have been three main hypotheses[46,189] attempting to explain this phenomenon: (1) Blindness eliminates abnormal visual percepts, which are able to disrupt visual perception and, therefore, mental models of the world created on its basis. (2) Visual impairment can improve some aspects of sensomotoric, olfactory, and auditory cognition—the modalities of perception that are disrupted by schizophrenia—and this causes a compensation effect. This effect can protect against schizophrenia only if the vision loss occurs within the first year of life. (3) Congenital blindness is also connected to a reduction in language flexibility and dynamic representation of the body, which probably provides a protective effect regarding the experience of the self. We propose a new (fourth) hypothesis that the blindness-mediated suppression of aberrant visual signals from the sensory periphery prevents the amplification of network instability in higher cortical areas.

CONCLUSION

The disruption of the early stages of visual processing and related mechanisms of higher visual cognition in schizophrenia patients has been described repeatedly. The incorrect integration of visual information occurs even in the early phase of visual perception. Visual information is subsequently coded into a specific pattern of neuronal signal. The disruption is detectable in both the retina and other segments of the visual cascade, such as the optic nerve, the LGN, and the V1.

In the early stages of the disease, and in untreated patients, hypersensitivity to LSFs has been documented. During the further course (and medication) of schizophrenia, this hypersensitivity turns into hyposensitivity and begins to affect other spatial frequencies of visual perception. Alterations to the visual signal, which are largely inconsistent over the course of schizophrenia (remission and relapse phases), may lead to the formation of inconsistent internal models of the world. These signal alterations (noise-to-signal ratios) are associated with fluctuations in DA and ACh levels, decreased activity of inhibitory GABAergic INs, and hypofunction of NMDAr associated with gradual loss of cell populations in the precortical visual circuit. The volatile and noisy signal from the periphery may then act as an amplifier of primarily decreased connectivity within frontal areas, which may then prograde retrogradely to lower cortical areas of the visual information processing circuit.

This assumption opens several important questions to be addressed in future studies. First, the role of disruptions in visual signal integration in the interactions between different regions of the precortical and cortical circuit should be elucidated. Second, the influence of error generation in regions of upstream visual pathways on the overall interaction among them should clarify the aberrant processing of visual information. Importantly, these errors could be cumulative, compensatory, or both. Third, the association between unstable signal from the visual periphery and gray matter loss in cortical areas should be verified. Answering these questions could identify novel possibilities for the treatment and remediation of schizophrenia. For example, specific modulation of the visual scene (noise, contrast, etc.) could be used to improve its integration within visual processing in schizophrenia patients or high-risk subjects by compensating for the initial steps of the pathophysiological cascade.

REFERENCES

1. Kalkstein, S., Hurford, I. & Gur, R. C. Neurocognition in schizophrenia. *Behavioral Neurobiology of Schizophrenia and its Treatment* **4**, 373–390 (2010).
2. Kar, S. K., Garg, K. & Tripathi, A. Olfactory hallucinations in schizophrenia: Does it carry any meaning? *Int. J. Nutr., Pharmacol., Neurol. Dis.* **6**, 136 (2016).
3. Chieffi, S. Dysfunction of magnocellular/dorsal processing stream in schizophrenia. *Curr. Psychiatry Res. Rev. Formerly: Curr. Psychiatry Rev.* **15**, 26–36 (2019).
4. Dondé, C., Avissar, M., Weber, M. M. & Javitt, D. C. A century of sensory processing dysfunction in schizophrenia. *Eur. Psychiatry* **59**, 77–79 (2019).
5. Javitt, D. C. & Freedman, R. Sensory processing dysfunction in the personal experience and neuronal machinery of schizophrenia. *Am. J. Psychiatry* **172**, 17–31 (2015).
6. Butler, P. D., Silverstein, S. M. & Dakin, S. C. Visual perception and its impairment in schizophrenia. *Biol. Psychiatry* **64**, 40–47 (2008).
7. Butler, P. D. et al. Early-stage visual processing and cortical amplification deficits in schizophrenia. *Arch. Gen. Psychiatry* **62**, 495–504 (2005).
8. Kéri, S., Kiss, I., Kelemen, O., Benedek, G. & Janka, Z. Anomalous visual experiences, negative symptoms, perceptual organization and the magnocellular pathway in schizophrenia: A shared construct? *Psychol. Med.* **35**, 1445 (2005).
9. Damilou, A., Apostolakis, S., Thrapsanioti, E., Theleritis, C. & Smyrnis, N. Shared and distinct oculomotor function deficits in schizophrenia and obsessive compulsive disorder. *Psychophysiology* **53**, 796–805 (2016).
10. Mather, J. A. Saccadic eye movements to seen and unseen targets: Oculomotor errors in normal subjects resembling those of schizophrenics. *J. Psychiatric Res.* **20**, 1–8 (1986).
11. Mather, J. A. & Putchat, C. Motor control of schizophrenics—I. Oculomotor control of schizophrenics: A deficit in sensory processing, not strictly in motor control. *J. Psychiatric Res.* **17**, 343–360 (1982).
12. Paštrnák, M., Dorazilová, A. & Rodriguez, M. Vizuální Percepce a Její Narušení U Schizofrenního Onemocnění-Přehledová Studie. *Ceskoslovenska Psychologie* **61**, 593–604 (2017).
13. Butler, P. D. et al. Dysfunction of early-stage visual processing in schizophrenia. *Am. J. Psychiatry* **158**, 1126–1133 (2001).
14. Chen, Y., Levy, D. L., Sheremata, S. & Holzman, P. S. Compromised late-stage motion processing in schizophrenia. *Biol. Psychiatry* **55**, 834–841 (2004).
15. Kogata, T. & Iidaka, T. A review of impaired visual processing and the daily visual world in patients with schizophrenia. *Nagoya J. Med. Sci.* **80**, 317 (2018).
16. Cutting, J. & Dunne, F. The nature of the abnormal perceptual experiences at the onset of schizophrenia. *Psychopathology* **19**, 347–352 (1986).
17. Hébert, M. et al. Retinal response to light in young nonaffected offspring at high genetic risk of neuropsychiatric brain disorders. *Biol. Psychiatry* **67**, 270–274 (2010).
18. Holzman, P. S. et al. Eye-tracking dysfunctions in schizophrenic patients and their relatives. *Arch. Gen. Psychiatry* **31**, 143–151 (1974).
19. Loughland, C. M., Williams, L. M. & Harris, A. W. Visual scanpath dysfunction in first-degree relatives of schizophrenia probands: Evidence for a vulnerability marker? *Schizophr. Res.* **67**, 11–21 (2004).
20. Schiffman, J. et al. Premorbid childhood ocular alignment abnormalities and adult schizophrenia-spectrum disorder. *Schizophr. Res.* **81**, 253–260 (2006).
21. Schubert, E., Henriksson, K. & McNeil, T. A prospective study of offspring of women with psychosis: Visual dysfunction in early childhood predicts schizophrenia-spectrum disorders in adulthood. *Acta Psychiatr. Scand.* **112**, 385–393 (2005).
22. Gottesman, I. I. & Gould, T. D. The endophenotype concept in psychiatry: Etymology and strategic intentions. *Am. J. Psychiatry* **160**, 636–645 (2003).
23. Chen, Y., Nakayama, K., Levy, D. L., Matthysse, S. & Holzman, P. S. Psychophysical isolation of a motion-processing deficit in schizophrenics and their relatives and its association with impaired smooth pursuit. *Proc. Natl Acad. Sci. USA* **96**, 4724–4729 (1999).
24. Phillipson, O. & Harris, J. Perceptual changes in schizophrenia: A questionnaire survey. *Psychol. Med.* **15**, 859–866 (1985).
25. Klosterkötter, J., Hellmich, M., Steinmeyer, E. M. & Schultze-Lutter, F. Diagnosing schizophrenia in the initial prodromal phase. *Arch. Gen. Psychiatry* **58**, 158–164 (2001).
26. Silverstein, S. M. Visual perception disturbances in schizophrenia: a unified model. *The Neuropsychopathology of Schizophrenia* **63**, 77–132 (2016).
27. Bar, M. et al. Top-down facilitation of visual recognition. *Proc. Natl Acad. Sci. USA* **103**, 449–454 (2006).
28. Panichello, M. F., Cheung, O. S. & Bar, M. Predictive feedback and conscious visual experience. *Front. Psychol.* **3**, 620 (2013).
29. Gordon, N., Tsuchiya, N., Koenig-Robert, R. & Hohwy, J. Expectation and attention increase the integration of top-down and bottom-up signals in perception through different pathways. *PLoS Biol.* **17**, e3000233 (2019).
30. Kauffmann, L., Ramanoël, S. & Peyrin, C. The neural bases of spatial frequency processing during scene perception. *Front. Integr. Neurosci.* **8**, 37 (2014).
31. Born, R. T. & Bencomo, G. M. Illusions, delusions, and your backwards bayesian brain: A biased visual perspective. *Brain, Behav. Evol.* **95**, 272–285 (2020).
32. Skottun, B. C. & Skoyles, J. R. Contrast sensitivity and magnocellular functioning in schizophrenia. *Vision Res.* **47**, 2923–2933 (2007).

33. Parr, T. & Friston, K. J. Attention or salience? *Curr. Opin. Psychol.* **29**, 1–5 (2019).

34. Roiser, J. et al. Do patients with schizophrenia exhibit aberrant salience? *Psychol. Med.* **39**, 199–209 (2009).

35. Silverstein, S. et al. Increased fusiform area activation in schizophrenia during processing of spatial frequency-degraded faces, as revealed by fMRI. *Psychol. Med.* **40**, 1159 (2010).

36. Butler, P. D. et al. An event-related potential examination of contour integration deficits in schizophrenia. *Front. Psychol.* **4**, 132 (2013).

37. Silverstein, S. M. et al. An fMRI examination of visual integration in schizophrenia. *J. Integr. Neurosci.* **8**, 175–202 (2009).

38. Dima, D. et al. Understanding why patients with schizophrenia do not perceive the hollow-mask illusion using dynamic causal modelling. *Neuroimage* **46**, 1180–1186 (2009).

39. Silverstein, S. M. et al. Perceptual organization and visual search processes during target detection task performance in schizophrenia, as revealed by fMRI. *Neuropsychologia* **48**, 2886–2893 (2010).

40. Martínez, A. et al. Magnocellular pathway impairment in schizophrenia: Evidence from functional magnetic resonance imaging. *J. Neurosci.* **28**, 7492–7500 (2008).

41. Clark, C. M., Gosselin, F. & Goghari, V. M. Aberrant patterns of visual facial information usage in schizophrenia. *J. Abnorm. Psychol.* **122**, 513 (2013).

42. Sehatpour, P. et al. Impaired visual object processing across an occipital-frontal-hippocampal brain network in schizophrenia: An integrated neuroimaging study. *Arch. Gen. Psychiatry* **67**, 772–782 (2010).

43. Silverstein, S. et al. Reduced top-down influences in contour detection in schizophrenia. *Cogn. Neuropsychiatry* **11**, 112–132 (2006).

44. Uhlhaas, P. J., Phillips, W. A., Mitchell, G. & Silverstein, S. M. Perceptual grouping in disorganized schizophrenia. *Psychiatry Res.* **145**, 105–117 (2006).

45. Butler, P. D. et al. Subcortical visual dysfunction in schizophrenia drives secondary cortical impairments. *Brain* **130**, 417–430 (2007).

46. Silverstein, S. et al. Vision in schizophrenia: Why it matters. *Front. Psychol.* **6**, 41 (2015).

47. de Lecea, L., Carter, M. E. & Adamantidis, A. Shining light on wakefulness and arousal. *Biol. Psychiatry* **71**, 1046–1052 (2012).

48. Shoshina, I. et al. The internal noise of the visual system and cognitive functions in schizophrenia. *Proc. Comput. Sci.* **169**, 813–820 (2020).

49. Silverstein, S. M., Fradkin, S. I. & Demmin, D. L. Schizophrenia and the retina: Towards a 2020 perspective. *Schizophr. Res.* **219**, 84–94 (2020).

50. Roy, S. & Field, G. D. Dopaminergic modulation of retinal processing from starlight to sunlight. *J. Pharmacol. Sci.* **140**, 86–93 (2019).

51. Herzog, M. H., Roinishvili, M., Chkonia, E. & Brand, A. Schizophrenia and visual backward masking: A general deficit of target enhancement. *Front. Psychol.* **4**, 254 (2013).

52. Uno, Y. & Coyle, J. T. Glutamate hypothesis in schizophrenia. *Psychiatry Clin. Neurosci.* **73**, 204–215 (2019).

53. Gazzaley, A. et al. Functional interactions between prefrontal and visual association cortex contribute to top-down modulation of visual processing. *Cerebral Cortex* **17**, i125–i135 (2007).

54. Griesmayr, B. et al. EEG theta phase coupling during executive control of visual working memory investigated in individuals with schizophrenia and in healthy controls. *Cogn., Affect., Behav. Neurosci.* **14**, 1340–1355 (2014).

55. Kane, M. J. et al. Individual differences in the executive control of attention, memory, and thought, and their associations with schizotypy. *J. Exp. Psychol.: Gen.* **145**, 1017 (2016).

56. Jiang, Y. et al. Progressive reduction in gray matter in patients with schizophrenia assessed with MR imaging by using causal network analysis. *Radiology* **287**, 633–642 (2018).

57. Takayanagi, Y. et al. Reduced cortical thickness in schizophrenia and schizotypal disorder. *Schizophr. Bull.* **46**, 387–394 (2020).

58. Vita, A., De Peri, L., Deste, G. & Sacchetti, E. Progressive loss of cortical gray matter in schizophrenia: A meta-analysis and meta-regression of longitudinal MRI studies. *Transl. Psychiatry* **2**, e190–e190 (2012).

59. Benes, F. M. Amygdalocortical circuitry in schizophrenia: From circuits to molecules. *Neuropsychopharmacology* **35**, 239–257 (2010).

60. Daenen, E. W., Wolterink, G., Van Der Heyden, J. A., Kruse, C. G. & Van Ree, J. M. Neonatal lesions in the amygdala or ventral hippocampus disrupt prepulse inhibition of the acoustic startle response; implications for an animal model of neurodevelopmental disorders like schizophrenia. *Eur. Neuropsychopharmacol.* **13**, 187–197 (2003).

61. Kalus, P., Muller, T. J., Zuschratter, W. & Senitz, D. The dendritic architecture of prefrontal pyramidal neurons in schizophrenic patients. *Neuroreport* **11**, 3621–3625 (2000).

62. Melicher, T. et al. White matter changes in first episode psychosis and their relation to the size of sample studied: A DTI study. *Schizophr. Res.* **162**, 22–28 (2015).

63. Venkatasubramanian, G., Jayakumar, P., Gangadhar, B. & Keshavan, M. Automated MRI parcellation study of regional volume and thickness of prefrontal cortex (PFC) in antipsychotic-naïve schizophrenia. *Acta Psychiatr. Scand.* **117**, 420–431 (2008).

64. Roska, B. & Meister, M. The Retina Dissects the Visual Scene. *The New Visual Neurosciences*, 163–182 (2014).

65. Demmin, D. L., Davis, Q., Roché, M. & Silverstein, S. M. Electroretinographic anomalies in schizophrenia. *J. Abnorm. Psychol.* **127**, 417 (2018).

66. Lee, W. W., Tajunisah, I., Sharmilla, K., Peyman, M. & Subrayan, V. Retinal nerve fiber layer structure abnormalities in schizophrenia and its relationship to disease state: evidence from optical coherence tomography. *Invest. Ophthalmol. Vis. Sci.* **54**, 7785–7792 (2013).

67. Silverstein, S. M. & Rosen, R. Schizophrenia and the eye. *Schizophr. Res.: Cogn.* **2**, 46–55 (2015).

68. Harris, J., Calvert, J., Leendertz, J. & Phillipson, O. The influence of dopamine on spatial vision. *Eye* **4**, 806–812 (1990).

69. Koizumi, A. et al. Atypical spatial frequency dependence of visual metacognition among schizophrenia patients. *NeuroImage: Clin.* **27**, 102296 (2020).

70. Samani, N. N. et al. Retinal layer abnormalities as biomarkers of schizophrenia. *Schizophr. Bull.* **44**, 876–885 (2018).

71. Archibald, N. K., Clarke, M. P., Mosimann, U. P. & Burn, D. J. Visual symptoms in Parkinson's disease and Parkinson's disease dementia. *Mov. Disord.* **26**, 2387–2395 (2011).

72. Urwyler, P. et al. Visual complaints and visual hallucinations in Parkinson's disease. *Parkinsonism Relat. Disord.* **20**, 318–322 (2014).

73. Brandies, R. & Yehuda, S. The possible role of retinal dopaminergic system in visual performance. *Neurosci. Biobehav. Rev.* **32**, 611–656 (2008).

74. ffytche, D. H. Visual hallucinations in eye disease. *Curr. Opin. Neurol.* **22**, 28–35 (2009).

75. Silverstein, S. M., Kovács, I., Corry, R. & Valone, C. Perceptual organization, the disorganization syndrome, and context processing in chronic schizophrenia. *Schizophr. Res.* **43**, 11–20 (2000).

76. Clark, M., Waters, F., Vatskalis, T. & Jablensky, A. On the interconnectedness and prognostic value of visual and auditory hallucinations in first-episode psychosis. *Eur. Psychiatry* **41**, 122–128 (2017).

77. Zhuo, C. et al. Antipsychotic agents deteriorate brain and retinal function in schizophrenia patients with combined auditory and visual hallucinations: A pilot study and secondary follow-up study. *Brain Behav.* **10**, e01611 (2020).

78. Zhuo, C. et al. Patients with first-episode untreated schizophrenia who experience concomitant visual disturbances and auditory hallucinations exhibit co-impairment of the brain and retinas-a pilot study. *Brain Imaging Behav.* **15**, 1–9 (2020).

79. Fallon, S. J., Zokaei, N. & Husain, M. Causes and consequences of limitations in visual working memory. *Ann. N. Y. Acad. Sci.* **1369**, 40 (2016).

80. Ascaso, F. J. et al. Retinal nerve fiber layer thickness measured by optical coherence tomography in patients with schizophrenia: A short report. *Eur. J. Psychiatry* **24**, 227–235 (2010).

81. Jerotić, S. & Marić, N. P. Structural retinal abnormalities as potential markers for psychosis spectrum disorders. *Medicinski Podmladak* **69**, 41–47 (2018).

82. Wannan, C. M. et al. Evidence for network-based cortical thickness reductions in schizophrenia. *Am. J. Psychiatry* **176**, 552–563 (2019).

83. Adams, S. A. & Nasrallah, H. A. Multiple retinal anomalies in schizophrenia. *Schizophr. Res.* **195**, 3–12 (2018).

84. Hosak, L., Sery, O., Sadykov, E. & Studnicka, J. Retinal abnormalitites as a diagnostic or prognostic marker of schizophrenia. *Biomed. Pap. Med. Fac. Palacky Univ. Olomouc* **162**, 159–164 (2018).

85. Bringmann, A., Grosche, A., Pannicke, T. & Reichenbach, A. GABA and glutamate uptake and metabolism in retinal glial (Müller) cells. *Front. Endocrinol.* **4**, 48 (2013).

86. Gracitelli, C. P. et al. Ophthalmology issues in schizophrenia. *Curr. Psychiatry Rep.* **17**, 28 (2015).

87. Hartwick, A. T., Hamilton, C. M. & Baldridge, W. H. Glutamatergic calcium dynamics and deregulation of rat retinal ganglion cells. *J. Physiol.* **586**, 3425–3446 (2008).

88. Reif, A. et al. A functional promoter polymorphism of neuronal nitric oxide synthase moderates prefrontal functioning in schizophrenia. *Int. J. Neuropsychopharmacol.* **14**, 887–897 (2011).

89. Silverstein, S. M. et al. Retinal microvasculature in schizophrenia. *Eye Brain* **13**, 205 (2021).

90. De Jong, F. J. et al. Arteriolar oxygen saturation, cerebral blood flow, and retinal vessel diameters: The Rotterdam Study. *Ophthalmology* **115**, 887–892 (2008).

91. Meier, M. H. et al. Microvascular abnormality in schizophrenia as shown by retinal imaging. *Am. J. Psychiatry* **170**, 1451–1459 (2013).

92. Sun, C., Wang, J. J., Mackey, D. A. & Wong, T. Y. Retinal vascular caliber: Systemic, environmental, and genetic associations. *Surv. Ophthalmol.* **54**, 74–95 (2009).

93. Huemer, K.-H. et al. Effects of dopamine on retinal and choroidal blood flow parameters in humans. *Br. J. Ophthalmol.* **91**, 1194–1198 (2007).

94. Lavoie, J. et al. The electroretinogram as a biomarker of central dopamine and serotonin: Potential relevance to psychiatric disorders. *Biol. Psychiatry* **75**, 479–486 (2014).

95. Hébert, M. et al. The electroretinogram may differentiate schizophrenia from bipolar disorder. *Biol. Psychiatry* **87**, 263–270 (2020).

96. Balogh, Z., Benedek, G. & Kéri, S. Retinal dysfunctions in schizophrenia. *Prog. Neuro-Psychopharmacol. Biol. Psychiatry* **32**, 297–300 (2008).

97. Gründer, G. & Cumming, P. *The Neurobiology of Schizophrenia* 109–124 (Elsevier, 2016).

98. Korshunov, K. S., Blakemore, L. J. & Trombley, P. Q. Dopamine: a modulator of circadian rhythms in the central nervous system. *Front. Cell. Neurosci.* **11**, 91 (2017).

99. Frazao, R. et al. Histamine elevates free intracellular calcium in mouse retinal dopaminergic cells via H1-receptors. *Invest. Ophthalmol. Vis. Sci.* **52**, 3083–3088 (2011).

100. Ortiz, G., Odom, J. V., Passaglia, C. L. & Tzekov, R. T. Efferent influences on the bioelectrical activity of the retina in primates. *Documenta Ophthalmol.* **134**, 57–73 (2017).

101. Nasser, J. A. et al. Electroretinographic detection of human brain dopamine response to oral food stimulation. *Obesity* **21**, 976–980 (2013).

102. Balasubramanian, R. & Gan, L. Development of retinal amacrine cells and their dendritic stratification. *Curr. Ophthalmol. Rep.* **2**, 100–106 (2014).

103. Veruki, M. L. & Wässle, H. Immunohistochemical localization of dopamine D receptors in rat retina. *Eur. J. Neurosci.* **8**, 2286–2297 (1996).

104. Biedermann, B., Fröhlich, E., Grosche, J., Wagner, H.-J. & Reichenbach, A. Mammalian Müller (glial) cells express functional D2 dopamine receptors. *Neuroreport* **6**, 609–612 (1995).

105. Veruki, M. L. Dopaminergic neurons in the rat retina express dopamine D2/3 receptors. *Eur. J. Neurosci.* **9**, 1096–1100 (1997).

106. Witkovsky, P. Dopamine and retinal function. *Documenta Ophthalmol.* **108**, 17–39 (2004).

107. Piccolino, M., Neyton, J. & Gerschenfeld, H. Decrease of gap junction permeability induced by dopamine and cyclic adenosine 3′: 5′-monophosphate in horizontal cells of turtle retina. *J. Neurosci.* **4**, 2477–2488 (1984).

108. Bloomfield, S. A. & Dacheux, R. F. Rod vision: Pathways and processing in the mammalian retina. *Prog. Retinal Eye Res.* **20**, 351–384 (2001).

109. Demb, J. B. & Singer, J. H. Intrinsic properties and functional circuitry of the AII amacrine cell. *Vis. Neurosci.* **29**, 51 (2012).

110. Daw, N. W., Brunken, W. J. & Jensen, R. J. *Neurobiology of the Inner Retina* 363–374 (Springer, 1989).

111. Li, H. et al. Adenosine and dopamine receptors coregulate photoreceptor coupling via gap junction phosphorylation in mouse retina. *J. Neurosci.* **33**, 3135–3150 (2013).

112. Jurišić, D. et al. New insights into schizophrenia: A look at the eye and related structures. *Psychiatr. Danub.* **32**, 60–69 (2020).

113. Qian, H. & Ripps, H. The GABAC receptors of retinal neurons. *Prog. Brain Res.* **131**, 295–308 (2001).

114. Copenhagen, D. R. & Jahr, C. E. Release of endogenous excitatory amino acids from turtle photoreceptors. *Nature* **341**, 536–539 (1989).

115. Javitt, D. C. Glutamate and schizophrenia: Phencyclidine, N-methyl-d-aspartate receptors, and dopamine–glutamate interactions. *Int. Rev. Neurobiol.* **78**, 69–108 (2007).

116. Phillips, W. A. & Silverstein, S. M. Convergence of biological and psychological perspectives on cognitive coordination in schizophrenia. *Behav. Brain Sci.* **26**, 65–82 (2003).

117. Uhlhaas, P. J., Millard, I., Muetzelfeldt, L., Curran, H. V. & Morgan, C. J. Perceptual organization in ketamine users: Preliminary evidence of deficits on night of drug use but not 3 days later. *J. Psychopharmacol.* **21**, 347–352 (2007).

118. Barnett, N. L. & Pow, D. V. Antisense knockdown of GLAST, a glial glutamate transporter, compromises retinal function. *Invest. Ophthalmol. Vis. Sci.* **41**, 585–591 (2000).

119. Bulens, C., Meerwaldt, J., Van Der Wildt, G. & Keemink, C. Visual contrast sensitivity in drug-induced Parkinsonism. *J. Neurol., Neurosurg. Psychiatry* **52**, 341–345 (1989).

120. Chen, Y. et al. Effects of typical, atypical, and no antipsychotic drugs on visual contrast detection in schizophrenia. *Am. J. Psychiatry* **160**, 1795–1801 (2003).

121. Domenici, L., Trimarchi, C., Piccolino, M., Fiorentini, A. & Maffei, L. Dopaminergic drugs improve human visual contrast sensitivity. *Hum. Neurobiol.* **4**, 195–197 (1985).

122. Kéri, S. & Benedek, G. Visual contrast sensitivity alterations in inferred magnocellular pathways and anomalous perceptual experiences in people at high-risk for psychosis. *Vis. Neurosci.* **24**, 183 (2007).

123. Zhang, A. J., Jacoby, R. & Wu, S. M. Light-and dopamine-regulated receptive field plasticity in primate horizontal cells. *J. Comp. Neurol.* **519**, 2125–2134 (2011).

124. Dowling, J. E. *The Retina: An Approachable Part of the Brain* (Harvard University Press, 1987).

125. Demmin, D. L., Mote, J., Beaudette, D. M., Thompson, J. L. & Silverstein, S. M. Retinal functioning and reward processing in schizophrenia. *Schizophr. Res.* **219**, 25–33 (2020).

126. Pelino, C. J. & Pizzimenti, J. J. The miniature multitasker: What makes the hypothalamus so important to the eye and visual system? *Rev. Optometry* **151**, 76–78 (2014).

127. Cao, D. et al. Functional loss in the magnocellular and parvocellular pathways in patients with optic neuritis. *Invest. Ophthalmol. Vis. Sci.* **52**, 8900–8907 (2011).

128. Casagrande, V. & Ichida, J. Processing in the lateral geniculate nucleus (LGN). *Adler's Physiology of the Eye* 574–585 (2011).

129. Casagrande, V.A. & Xu, X. Parallel visual pathways: a comparative perspective. *The Visual Neurosciences*, 494–506 (MIT Press, 2004).

130. Sherman, S. M. & Guillery, R. W. *Exploring the Thalamus and its Role in Cortical Function* (MIT Press, 2006).

131. Krueger, J. & Disney, A. A. Structure and function of dual-source cholinergic modulation in early vision. *J. Comp. Neurol.* **527**, 738–750 (2019).

132. Casagrande, V. A., Royal, D. W. & Sáry, G. Extraretinal inputs and feedbackmechanisms to the lateral geniculate nucleus (LGN). *The Primate Visual System: A Comparative Approach*, 191–211 (2005).

133. García-Cabezas, M. Á., Martínez-Sánchez, P., Sánchez-González, M. Á., Garzón, M. & Cavada, C. Dopamine innervation in the thalamus: Monkey versus rat. *Cerebral Cortex* **19**, 424–434 (2009).

134. Zhao, Y., Kerscher, N., Eysel, U. & Funke, K. D1 and D2 receptor-mediated dopaminergic modulation of visual responses in cat dorsal lateral geniculate nucleus. *J. Physiol.* **539**, 223–238 (2002).

135. Godwin, D. W., Vaughan, J. W. & Sherman, S. M. Metabotropic glutamate receptors switch visual response mode of lateral geniculate nucleus cells from burst to tonic. *J. Neurophysiol.* **76**, 1800–1816 (1996).

136. Nakajima, M., Schmitt, L. I. & Halassa, M. M. Prefrontal cortex regulates sensory filtering through a basal ganglia-to-thalamus pathway. *Neuron* **103**, 445–458. e410 (2019).

137. Varela, C. Thalamic neuromodulation and its implications for executive networks. *Front. Neural Circuits* **8**, 69 (2014).

138. Stidwill, D. & Fletcher, R. *Normal Binocular Vision: Theory, Investigation and Practical Aspects* (John Wiley & Sons, 2017).

139. Poltoratski, S., Maier, A., Newton, A. T. & Tong, F. Figure-ground modulation in the human lateral geniculate nucleus is distinguishable from top-down attention. *Curr. Biol.* **29**, 2051–2057. e2053 (2019).

140. Xu, X. et al. A comparison of koniocellular, magnocellular, and parvocellular receptive field properties in the lateral geniculate nucleus of the owl monkey (Aotus trivirgatus). *J. Physiol.* **531**, 203–218 (2001).

141. Kim, U. S., Mahroo, O. A., Mollon, J. D. & Yu-Wai-Man, P. Retinal ganglion cells-diversity of cell types and clinical relevance. *Front. Neurol.* **12**, 661938 (2021).

142. Yan, W. et al. Cell atlas of the human fovea and peripheral retina. *Sci. Rep.* **10**, 1–17 (2020).

143. Cao, D., Lee, B. B. & Sun, H. Combination of rod and cone inputs in parasol ganglion cells of the magnocellular pathway. *J. Vis.* **10**, 4–4 (2010).

144. Marosi, C., Fodor, Z. & Csukly, G. From basic perception deficits to facial affect recognition impairments in schizophrenia. *Sci. Rep.* **9**, 1–13 (2019).

145. Shoshina, I., Mukhitova, Y. V., Tregubenko, I., Pronin, S. & Isaeva, E. Contrast sensitivity of the visual system and cognitive functions in schizophrenia and depression. *Human Physiol.* **47**, 516–527 (2021).

146. Vaziri-Pashkam, M., Taylor, J. & Xu, Y. Spatial frequency tolerant visual object representations in the human ventral and dorsal visual processing pathways. *J. Cogn. Neurosci.* **31**, 49–63 (2019).

147. Skottun, B. C. On the use of spatial frequency to isolate contributions from the magnocellular and parvocellular systems and the dorsal and ventral cortical streams. *Neurosci. Biobehav. Rev.* **56**, 266–275 (2015).

148. Dacey, D. The mosaic of midget ganglion cells in the human retina. *J. Neurosci.* **13**, 5334–5355 (1993).

149. Kling, A., Field, G., Brainard, D. & Chichilnisky, E. Probing computation in the primate visual system at single-cone resolution. *Annu. Rev. Neurosci.* **42**, 169–186 (2019).

150. Patterson, S. S. et al. Another blue-ON ganglion cell in the primate retina. *Curr. Biol.* **30**, R1409–R1410 (2020).

151. Hall, N. & Colby, C. Psychophysical definition of S-cone stimuli in the macaque. *J. Vis.* **13**, 20–20 (2013).

152. Hall, N. & Colby, C. S-cone visual stimuli activate superior colliculus neurons in old world monkeys: Implications for understanding blindsight. *J. Cogn. Neurosci.* **26**, 1234–1256 (2014).

153. Hall, N. J. & Colby, C. L. Express saccades and superior colliculus responses are sensitive to short-wavelength cone contrast. *Proc. Natl Acad. Sci. USA* **113**, 6743–6748 (2016).

154. Kveraga, K., Im, H. Y., Ward, N. & Adams, R. B. Fast saccadic and manual responses to faces presented to the koniocellular visual pathway. *J. Vis.* **20**, 9–9 (2020).

155. Enroth-Cugell, C. & Robson, J. G. Functional characteristics and diversity of cat retinal ganglion cells. Basic characteristics and quantitative description. *Invest. Ophthalmol. Vis. Sci.* **25**, 250–267 (1984).

156. Welbourne, L. E., Morland, A. B. & Wade, A. R. Population receptive field (pRF) measurements of chromatic responses in human visual cortex using fMRI. *NeuroImage* **167**, 84–94 (2018).

157. Marc, Robert E. Synaptic organization of the retina. *Adler's Physiology of the Eye*. 443-458, (Philadelphia: Saunders Elsevier, 2011).

158. Yang, C. R. & Seamans, J. K. Dopamine D1 receptor actions in layers V-VI rat prefrontal cortex neurons in vitro: modulation of dendritic-somatic signal integration. *J. Neurosci.* **16**, 1922–1935 (1996).

159. Bennett, C. et al. Higher-order thalamic circuits channel parallel streams of visual information in mice. *Neuron* **102**, 477–492. e475 (2019).

160. Parnaudeau, S., Bolkan, S. S. & Kellendonk, C. The mediodorsal thalamus: An essential partner of the prefrontal cortex for cognition. *Biol. Psychiatry* **83**, 648–656 (2018).

161. Maith, O., Schwarz, A. & Hamker, F. H. Optimal attention tuning in a neuro-computational model of the visual cortex–basal ganglia–prefrontal cortex loop. *Neural Netw.* **142**, 534–547 (2021).

162. Vuilleumier, P. Affective and motivational control of vision. *Curr. Opin. Neurol.* **28**, 29–35 (2015).

163. Hirata, A., Aguilar, J. & Castro-Alamancos, M. A. Noradrenergic activation amplifies bottom-up and top-down signal-to-noise ratios in sensory thalamus. *J. Neurosci.* **26**, 4426–4436 (2006).

164. Bar, M. A cortical mechanism for triggering top-down facilitation in visual object recognition. *J. Cogn. Neurosci.* **15**, 600–609 (2003).

165. Tapia, E. & Breitmeyer, B. G. Visual consciousness revisited: Magnocellular and parvocellular contributions to conscious and nonconscious vision. *Psychol. Sci.* **22**, 934–942 (2011).

166. Lee, T. S. Computations in the early visual cortex. *J. Physiol.-Paris* **97**, 121–139 (2003).

167. Kwon, H. et al. Early cortical signals in visual stimulus detection. *Neuroimage* **244**, 118608 (2021).

168. Wunderlich, K., Beierholm, U. R., Bossaerts, P. & O'Doherty, J. P. The human prefrontal cortex mediates integration of potential causes behind observed outcomes. *J. Neurophysiol.* **106**, 1558–1569 (2011).

169. Hamker, F. H. The reentry hypothesis: The putative interaction of the frontal eye field, ventrolateral prefrontal cortex, and areas V4, IT for attention and eye movement. *Cerebral Cortex* **15**, 431–447 (2005).

170. Noudoost, B. & Moore, T. Control of visual cortical signals by prefrontal dopamine. *Nature* **474**, 372–375 (2011).

171. Zhang, Y. et al. Object decoding with attention in inferior temporal cortex. *Proc. Natl Acad. Sci. USA* **108**, 8850–8855 (2011).

172. Dima, D., Dietrich, D. E., Dillo, W. & Emrich, H. M. Impaired top-down processes in schizophrenia: A DCM study of ERPs. *NeuroImage* **52**, 824–832 (2010).

173. Yang, E. et al. Visual context processing in schizophrenia. *Clin. Psychol. Sci.* **1**, 5–15 (2013).

174. Forbes, N., Carrick, L., McIntosh, A. & Lawrie, S. Working memory in schizophrenia: A meta-analysis. *Psychol. Med.* **39**, 889–905 (2009).

175. Guo, J., Ragland, J. D. & Carter, C. S. Memory and cognition in schizophrenia. *Mol. Psychiatry* **24**, 633–642 (2019).

176. Calderone, D. J. et al. Contributions of low and high spatial frequency processing to impaired object recognition circuitry in schizophrenia. *Cerebral Cortex* **23**, 1849–1858 (2013).

177. Marwick, K. & Hall, J. Social cognition in schizophrenia: A review of face processing. *Br. Med. Bull.* **88**, 43–58 (2008).

178. Anticevic, A., Repovs, G., Corlett, P. R. & Barch, D. M. Negative and nonemotional interference with visual working memory in schizophrenia. *Biol. Psychiatry* **70**, 1159–1168 (2011).

179. Stäblein, M. et al. Visual working memory encoding in schizophrenia and first-degree relatives: Neurofunctional abnormalities and impaired consolidation. *Psychol. Med.* **49**, 75–83 (2019).

180. Jahshan, C., Wolf, M., Karbi, Y., Shamir, E. & Rassovsky, Y. Probing the magnocellular and parvocellular visual pathways in facial emotion perception in schizophrenia. *Psychiatry Res.* **253**, 38–42 (2017).

181. O'Callaghan, C., Kveraga, K., Shine, J. M., Adams, R. B. Jr. & Bar, M. Predictions penetrate perception: Converging insights from brain, behaviour, and disorder. *Consciousness Cogn.* **47**, 63–74 (2017).

182. Corlett, P. R., Honey, G. D. & Fletcher, P. C. Prediction error, ketamine, and psychosis: An updated model. *J. Psychopharmacol.* **30**, 1145–1155 (2016).

183. Alexander, W. H. & Brown, J. W. Frontal cortex function as derived from hierarchical predictive coding. *Sci. Rep.* **8**, 1–11 (2018).

184. Inan, M., Petros, T. J. & Anderson, S. A. Losing your inhibition: Linking cortical GABAergic interneurons to schizophrenia. *Neurobiol. Dis.* **53**, 36–48 (2013).

185. Shaw, A. D. et al. Oscillatory, computational, and behavioral evidence for impaired GABAergic inhibition in schizophrenia. *Schizophr. Bull.* **46**, 345–353 (2020).

186. Leivada, E. Vision, language and a protective mechanism towards psychosis. *Neurosci. Lett.* **617**, 178–181 (2016).

187. Morgan, V. A. et al. Congenital blindness is protective for schizophrenia and other psychotic illness. A whole-population study. *Schizophr. Res.* **202**, 414–416 (2018).

188. Silverstein, S. M. et al. Effects of short-term inpatient treatment on sensitivity to a size contrast illusion in first-episode psychosis and multiple-episode schizophrenia. *Front. Psychol.* **4**, 466 (2013).

189. Landgraf, S. & Osterheider, M. "To see or not to see: that is the question". The "Protection-Against-Schizophrenia" (PaSZ) model: Evidence from congenital blindness and visuo-cognitive aberrations. *Front. Psychol.* **4**, 352 (2013).

AUTHOR CONTRIBUTIONS

FUNDING

COMPETING INTERESTS
The authors declare no competing interests.

ADDITIONAL INFORMATION
Correspondence and requests for materials should be addressed to Petr Adámek.

Reprints and permission information is available at http://www.nature.com/reprints

Publisher's note Springer Nature remains neutral with regard to jurisdictional claims in published maps and institutional affiliations.

Schizophrenia

ARTICLE   OPEN

The Gaze of Schizophrenia Patients Captured by Bottom-up Saliency

Petr Adámek [1,2] ✉, Dominika Grygarová[1,2], Lucia Jajcay[1,3,4], Eduard Bakštein[5,6], Petra Fürstová[5], Veronika Juríčková [1,7], Juraj Jonáš[1,8], Veronika Langová[1,2], Iryna Neskoroďana[1], Ladislav Kesner[1,9] and Jiří Horáček [1,2]

Schizophrenia (SCHZ) notably impacts various human perceptual modalities, including vision. Prior research has identified marked abnormalities in perceptual organization in SCHZ, predominantly attributed to deficits in bottom-up processing. Our study introduces a novel paradigm to differentiate the roles of top-down and bottom-up processes in visual perception in SCHZ. We analysed eye-tracking fixation ground truth maps from 28 SCHZ patients and 25 healthy controls (HC), comparing these with two mathematical models of visual saliency: one bottom-up, based on the physical attributes of images, and the other top-down, incorporating machine learning. While the bottom-up (GBVS) model revealed no significant overall differences between groups (beta = 0.01, $p = 0.281$, with a marginal increase in SCHZ patients), it did show enhanced performance by SCHZ patients with highly salient images. Conversely, the top-down (EML-Net) model indicated no general group difference (beta = −0.03, $p = 0.206$, lower in SCHZ patients) but highlighted significantly reduced performance in SCHZ patients for images depicting social interactions (beta = −0.06, $p < 0.001$). Over time, the disparity between the groups diminished for both models. The previously reported bottom-up bias in SCHZ patients was apparent only during the initial stages of visual exploration and corresponded with progressively shorter fixation durations in this group. Our research proposes an innovative approach to understanding early visual information processing in SCHZ patients, shedding light on the interplay between bottom-up perception and top-down cognition.

INTRODUCTION

Schizophrenia (SCHZ) is typically associated with deficits in domains related to information processing, such as perception, attention, working memory, and learning[1]. All these domains likely have one common denominator: impaired salience, the property by which something stands out from surrounding context. Salience is typically regarded as having two components: physical and cognitive salience. Physical salience refers to the aspects of a stimulus that automatically capture attention or direct gaze in a stimulus-driven, goal-independent, or bottom-up manner[2]. In contrast, cognitive salience is task-oriented, influenced by tasks assigned by external sources or driven by one's current internal goals[3]. Disruption of physical salience, which is based on sensory sensitivity to external stimuli, may impede the formation of cognitive salience-related associations. This means that it can affect our ability to attribute meaning to individual stimuli from the external environment[4]. Kapur proposed that dysregulated, hyperdopaminergic states at the cellular level may lead to the attribution of aberrant salience to individual experiences at the psychological experiential level[5]. However, salience formation is a complex, long-term process that reflects our internal model of the world, which may not be stable in SCHZ due to distortions and instability of sensory signals[6].

Vision is our most developed sense[7,8] and unsurprisingly a substantial amount of brain processing is devoted to it, with over half the primate brain being involved in vision-related processing[9]. Due to the limited computational capacity of the visual cortex[10], it is critical to correctly cluster visual percepts according to a hierarchy of importance. The internal model of the world is derived from the combination of neural filters and cognitive signals that gradually calibrate them. This mechanism allows the brain to process visual signals efficiently and to focus its limited computational capacity and attention only on those parts of the scene that are subconsciously assessed as important[11,12]. Computational capacity limits are mainly related to the physiological aspects of the neurons themselves and the functional circuits sensitive to the different elements of the visual scene[13,14]. The brain solves this limited capacity for attention allocation through prediction mechanisms[15]. The perceptual onset is preceded by a quick subliminal observation of the scene (bottom-up), which is based on its physical saliency (contrast, brightness, and low spatial frequencies). This observation helps us quickly orient ourselves and focus our attention in the next step, in which higher (top-down) cognitive processes come into play. These processes are related to the cognitive saliency formed by our internal model of the world[6,16]. Low spatial frequency (LSF) information is swiftly extracted from visual stimuli and conveys general details about the shape and orientation of objects within a scene. This LSF information subsequently contributes to the formation of top-down predictions, influencing visual attention and higher-level cognitive processes related to visual perception[16–19]. A primary outcome resulting from the disruption of this process is a disorder of attentional capacity and the inability to rapidly incorporate salient percepts into the stream of consciousness[20,21].

In SCHZ, previous findings indicated a disruption in both types of processing: basal visual perception based on incorrect

[1]Center for Advanced Studies of Brain and Consciousness, National Institute of Mental Health, Klecany, Czech Republic. [2]Third Faculty of Medicine, Charles University, Prague, Czech Republic. [3]Institute of Computer Science of the Czech Academy of Sciences, Prague, Czech Republic. [4]Faculty of Electrical Engineering, Czech Technical University in Prague, Prague, Czech Republic. [5]Early Episodes of SMI Research Center, National Institute of Mental Health, Klecany, Czech Republic. [6]Department of Cybernetics, Faculty of Electrical Engineering, Czech Technical University, Prague, Czech Republic. [7]First Faculty of Medicine, Charles University, Prague, Czech Republic. [8]Faculty of Humanities, Charles University, Prague, Czech Republic. [9]Department of Art History, Masaryk University, Brno, Czech Republic. ✉email: petr.adamek@nudz.cz

processing of visual stimuli (bottom-up)[22–25], and impairment of higher visual cognition based on the processing of visual stimuli influenced and orchestrated by previous experience (top-down/feedforward sweep)[26–34]. The stimuli used in these experiments are typically designed based on the research question being addressed. Bottom-up experiments predominantly work with elementary stimuli, such as basic line figures[35], Gabor patterns[29,36], and pop-out structures[37], while top-down experiments use different types of visual illusions[33,38] or faces[39]. However, this approach falls short in providing a comprehensive mapping of the interplay between bottom-up and top-down processes during complex visual processing in everyday environments. It also lacks the capability to conclusively ascertain how deficits in bottom-up processing influence the perception, cognition and formation of aberrant saliency of complex real-life scenes in SCHZ population.

To address this knowledge gap, we attempt to identify differences between both groups by using recent saliency "bottom-up" and "top-down" predictive models[40,41], with the former relying solely on physical visual properties and the latter additionally incorporating object recognition. Attention allocation has been intensively investigated through saliency models using "saliency maps"[42–44], a computational concept that predicts graded saliency for each location of an image based on its low-level visual features, and thus predicts bottom-up attention[45]. It includes three components: (1) feature maps that represent fundamental visual characteristics such as color, orientation, luminance, and motion; (2) saliency maps resulting from combining normalized feature maps that highlight the visually significant areas in an image, solely based on their physical attributes, without taking into account any semantic features of the stimulus; (3) the "ground truth maps" representing the saliency maps derived from the real eye-tracking data capturing viewer attention allocation to specific regions of the image. The efficacy of saliency model predictions is then evaluated through its comparison with ground truth maps. In previous studies, saliency models have even been employed to analyze brain activity in response to visual stimuli, with distinct brain areas linked to the 'saliency map' generated by a saliency model[46,47].

Recent technological advances in the field of machine learning have enabled the incorporation of additional convolutional neural network (CNN) layers to original bottom-up models. These added CNN layers reflect top-down cognition, which is involved in analysis and categorization of specific semantic content of a scene (e.g., objects, faces, emotions)[48–51]. However, it is important to emphasize that such models are not solely based on top-down cognition; they still incorporate the bottom-up layer within their computations. In this paper, for the sake of simplicity, we refer to such models as "top-down" because, unlike bottom-up models, they have the capability to suppress the bottom-up component in favour of top-down processing[52,53].

We utilized these two models to determine the likelihood of an observer directing their attention to specific areas within the scene. We expect that analyzing ground truth maps derived from eye-tracking data of individuals with schizophrenia (SCHZ) and healthy controls (HCs), and comparing these with mathematically predicted saliency, will provide deeper insights into the similarities and differences in bottom-up and top-down visual processing between these two groups. We hypothesized that SCHZ patients' attention is influenced more by the physical properties of the image than HC's attention. This suggests a tendency to prioritize highly physically salient percepts in the scene more than HC[54–57], likely reflecting the disruption of higher cortical processes consistently found across studies and resulting in the expected lower predictive ability of the top-down model in SCHZ patients[58–60]. In this paper, we employ the term "bottom-up bias" to denote a tendency to prioritize bottom-up signal over top-down processing[61].

To investigate the 'bottom-up bias' in schizophrenia (SCHZ), our approach involved a multi-faceted comparison using saliency models across both SCHZ patients and HCs. Initially, we compared the overall results of these models between the two groups. Furthermore, our analysis extended to assessing the performance of the saliency models across five specific content-based categories, each inherently linked to either bottom-up or top-down processing. This nuanced categorization allowed us to parse the visual processing mechanisms more precisely and understand how each model interprets different types of visual stimuli in SCHZ and HCs. Subsequently, we integrated a stepwise analysis of two consecutive time periods in our study – the first encompassing up to five fixations, and the second starting from the sixth fixation. This sequential analysis was aimed to unravel the dynamics of visual perception in SCHZ. By examining these two distinct phases, we sought to identify and contrast the engagement of bottom-up and top-down components in the visual perception processing of both groups. Finally, to reveal confounding factors that might influence the results of the two saliency models, we decided to test the relationship of oculomotor movements with psychological metrics (Continuous Performance Test (CPT) and Positive and Negative Syndrome Scale (PANSS)), medication, disease duration, and the length of its untreated phase (DUP).

RESULTS

Differences in the Performance of Saliency Models

Comparison of saliency maps calculated for each participant (ground truth maps) to saliency predictions lead to 13,436 normalized scan path (NSS) values from 53 subjects (28 SCHZ, 25 HC). A direct nonstatistical comparison of the NSS scores between two saliency models showed that the bottom-up (GBVS) model was able to predict oculomotor behavior better in the SCHZ population ($M = 1.43$, $SD = 0.58$) than in HC ($M = 1.35$, $SD = 0.51$). In contrast, the top-down (EML-Net) model better predicted the distribution of fixations in HC (HC: $M = 2.16$, $SD = 1.13$) than SCHZ (SCHZ: $M = 2.08$, $SD = 1.29$). However, when we employed linear mixed effects models (LME) for statistical comparison, the analysis did not corroborate the differences observed in the direct, nonstatistical comparison of NSS scores between groups and across models.

Evaluation of NSS scores for the bottom-up (GBVS) model did not show significant differences between-groups but indicated significantly higher performance of SCHZ patients in the highly salient image category (Table 1). The top-down (EML-Net) model also did not show an overall between-groups effect but showed significantly lower patients' performance in images depicting social interactions (Table 1).

At the whole-group level, including both SCHZ and HC, the bottom-up (GBVS) model showed no differences between image categories. On the other hand, the top-down (EML-Net) model showed lower prediction capability in the physically salient image category, and higher capability in the social interaction and social landscape image categories (Table 1).

Between-group differences in bottom-up and top-down predictions in time

To identify the inter-group differences in the involvement of bottom-up and top-down processes over time, we calculated NSS score for each model in two different time periods: up to the fifth fixation and from the sixth fixation (Fig. 1). The decision to split the dataset into two periods was based on previous research showing that prediction accuracy for bottom-up models is lost around the fifth fixation[62]. Another decision that led us to split the dataset is the peak of the fixation duration, which is located just around the fifth fixation, for both groups (Fig. 2). We applied LMER models to both periods and both saliency models.

Table 1. Results of LME comparison for top-down and bottom-up model.

Predictors	bottom-up sqrt(NSS)			top-down sqrt(NSS)		
	Estimates	CI	p	Estimates	CI	p
(Intercept)	0.44	0.37–0.58	<0.001	0.57	0.53–0.61	<0.001
SCHZ	0.01	−0.01–0.03	0.281	−0.03	−0.07–0.02	0.206
Incongruent	0.01	−0.10–0.11	0.921	0.04	−0.01–0.09	0.132
Physically salient	−0.04	−0.14–0.06	0.428	−0.11	−0.17−−0.06	<0.001
Social interaction	−0.08	−0.18–0.02	0.099	0.18	0.12–0.23	<0.001
Social landscape	−0.02	−0.12–0.08	0.699	0.09	0.04–0.14	0.001
SCHZ × Incongruent	0.01	−0.01–0.02	0.224	0.03	−0.00–0.06	0.050
SCHZ × Physically salient	0.02	0.00–0.03	0.015	0.03	−0.00–0.06	0.051
SCHZ × Social interaction	0.01	−0.01–0.02	0.324	−0.06	−0.09−−0.03	<0.001
SCHZ × Social landscape	0.01	−0.00–0.03	0.153	0.01	−0.02–0.04	0.582
Random Effects						
σ^2	0.02			0.07		
τ_{00}	0.00 ID			0.01 ID		
	0.00 imageCat			0.00 imageCat		
ICC	0.10			0.07		
N	54 ID			54 ID		
	5 imageCat			5 imageCat		
Observations	13436			13436		
Marginal R^2/Conditional R^2	0.049/0.140			0.090/0.157		

sqrt square root, NSS normalised scan path, ID unique participant identification string, imageCat Image category.

Sequential analysis of bottom-up (GBVS) model. The LME model revealed no significant differences in NSS scores between the SCHZ and HC groups for either observed period. However, in the context of physically salient images, the model consistently showed a better prediction of oculomotor behavior for SCHZ patients compared to HCs, in both periods (Table 2).

Furthermore, an analysis of the second period revealed differential performance across image categories at the whole-group level. Specifically, the bottom-up model indicated better performance for physically salient images, while it showed reduced effectiveness in accurately predicting oculomotor movements for stimuli depicting social interactions and social landscapes (Table 2).

Sequential analysis of top-down (EML-Net) model. LME results showed a difference in NSS score between groups during the first time period (Table 3). We also observed significantly higher model predictive performance of patients' oculomotor behavior in the physically salient image category and lower performance in social landscape images category in the first period. Stimuli depicting social interactions had significantly lower NSS score in SCHZ patients in both periods (Table 3). Contrastingly, when we examined the whole-group level results, which include both SCHZ and HC groups, no differences were observed between image categories in either of the two periods (Table 3).

Group Differences in Fixation and Explored Area of the Image

The SCHZ group showed a significantly lower mean number of fixations per image than the HC (SCHZ: M = 8.92, SD = 1.28; HC: M = 9.22, SD = 0.75; t(54) = 5.26, p < 0.001), and the overall mean fixation duration was longer in SCHZ than in HC (SCHZ: M = 326.12 ms, SD = 22.97; HC: M = 254.83 ms, SD = 24.15; t(54) = −4.44, p < 0.001). We also observed a statistically significant difference between the groups in terms of the total area of the image that received fixations. This 'total fixed image area' refers to the cumulative portion of the image that was the focus of gaze fixations across all participants within each group. The standard deviation (SD) test revealed that the SCHZ group had significantly reduced spread of fixations over the image area (SCHZ: SD Mean = 678.28; SD = 76.3; HC: SD Mean = 727.56 (SD = 83.82); t(54) = 6.87, p < 0.001).

In addition, we identified between-group differences in the temporal dynamics of fixation duration. In SCHZ, the average fixation duration stabilized after an initial increase in duration. Around the fifteenth fixation, their duration became comparable to HC. The fifth fixation was achieved in 99% of all trials in HC and in 96% of all trials in SCHZ. Tenth fixation was achieved in 96% of all trials in HC and in 82% of all trials in SCHZ. Fifteenth fixation was achieved in 79% of all trials in HC and in 45% of all trials in SCHZ. A sequential testing procedure was used to test the significance of this difference. The first fourteen fixations showed a statistically significant difference in fixation lengths (t(54) = −2.55, p = 0.013). The fifteenth and subsequent fixation durations did not differ between groups (t(54) = −1.67, p = 0.098) (Fig. 2).

In the SCHZ group, we also investigated the relationship between oculomotor movements (including the duration and number of fixations) and various factors: the antipsychotic medication dosage, responses on the PANSS questionnaire, the duration of illness, and the period of untreated illness. However, our analysis revealed no statistically significant correlations between these variables and oculomotor movements. Additionally, we examined the relationship between oculomotor movements and CPT test results in both SCHZ and HC groups. We found a negative correlation between CPT Commissions and the mean number of fixations in HC group, but no other significant correlations with other measured variables and participant groups. Detailed results can be found in (Table 4).
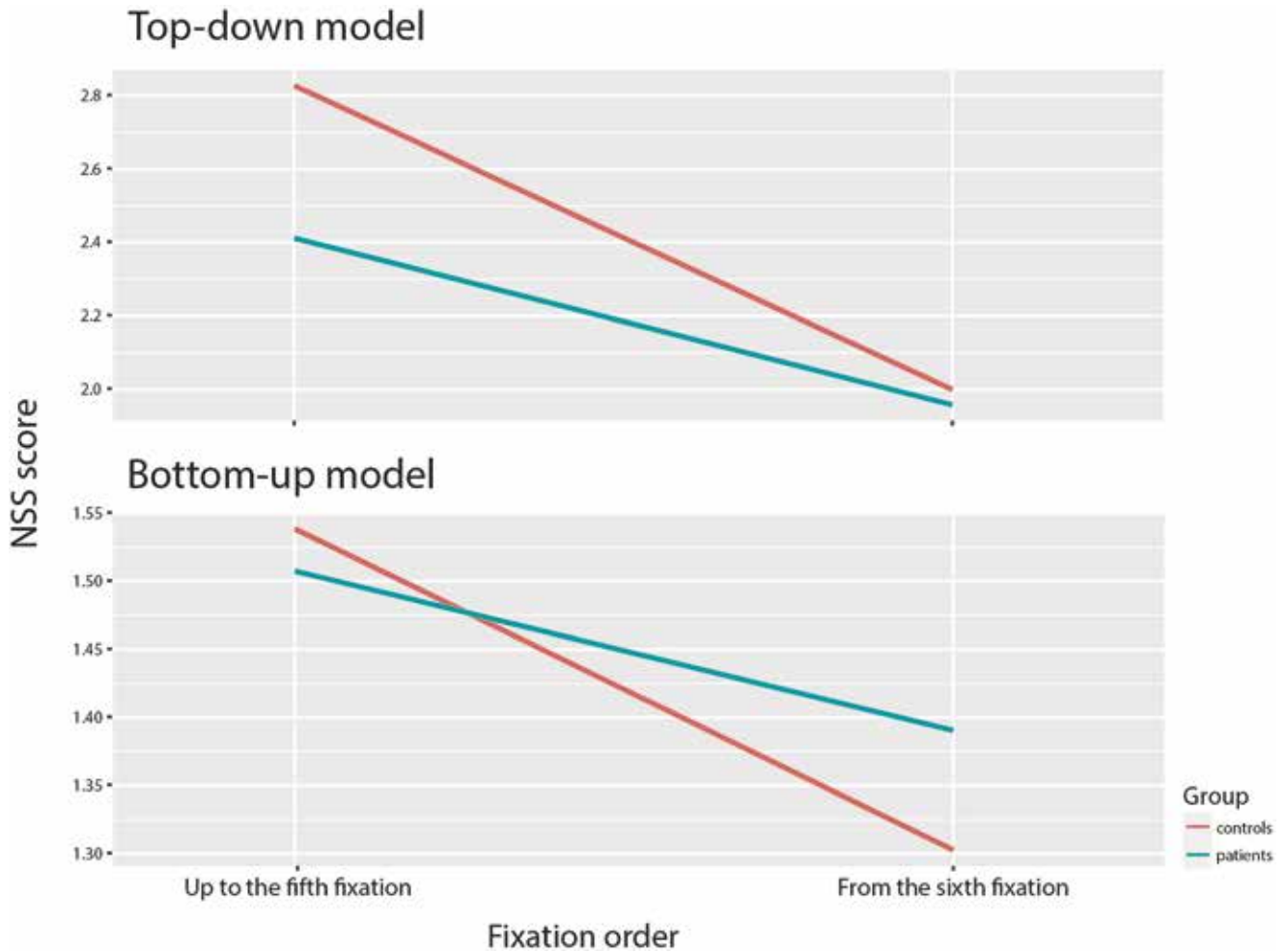
Fig. 1 The difference between models performance in time. A difference in NSS score of the top-down and bottom-up model between-groups over time. **Description:** The top-down (EML-Net) model performs better within both time periods in the case of HCs. The bottom-up model, on the other hand, is better in predicting saliency in the SCHZ population only in the case of the second period from the sixth fixation. In the first period, the prediction is more accurate for HCs than SCHZ patients.
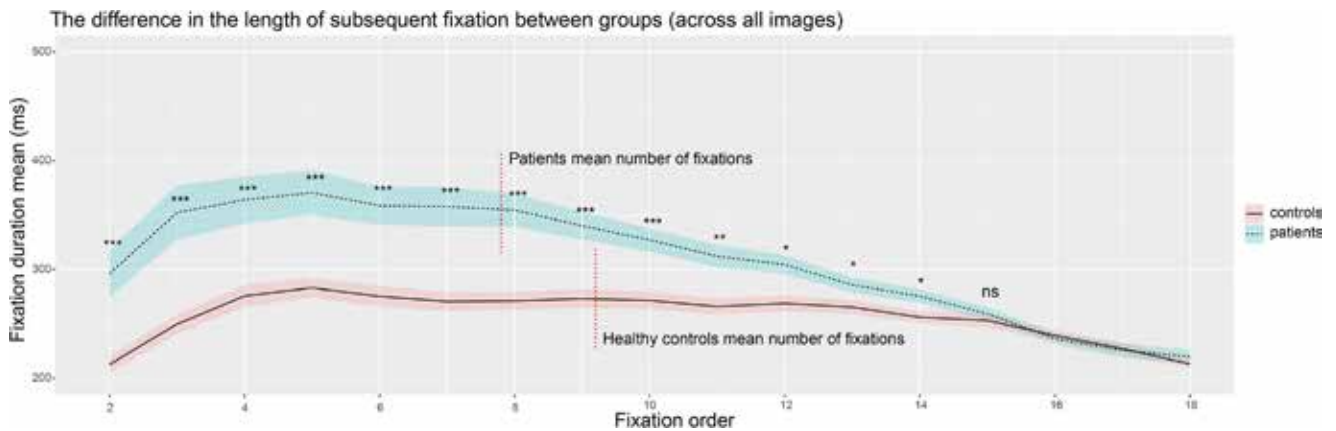

Fig. 2 Inter-group differences in the duration of individual fixations (group mean, standard error of the mean). Vertical red dotted lines show the mean number of fixations in groups ***$p < 0.001$; **$p < 0.01$; *$p < 0.05$; ns = not significant. A sequential testing procedure was applied to control false positive rate – stopping at the first fixation with a non-significant result.

DISCUSSION

The main finding of our study is that the bottom-up model was able to better predict the oculomotor behavior of the SCHZ population and in contrast the top-down model better predicted the oculomotor behavior of HCs. While the LME model did not statistically confirm differences for either the bottom-up or top-down models overall, it identified significant variations upon examining specific image categories. These findings indicate that

Table 2. Differences in NSS scores between SCHZ and HC groups, for bottom-up (GBVS) model in two different time periods.

Predictors	bottom-up sqrt(NSS) – To the fifth fixation			bottom-up sqrt(NSS) – Up to sixth fixation		
	Estimates	CI	p	Estimates	CI	p
(Intercept)	1.61	1.51–1.70	<0.001	1.54	1.52–1.57	<0.001
SCHZ	−0.02	−0.04–0.00	0.093	0.01	−0.0–0.04	0.270
Incongruent	0.03	−0.10–0.16	0.622	−0.00	−0.03–0.03	0.953
Physically salient	−0.06	−0.19–0.07	0.393	0.04	−0.07–−0.02	0.002
Social interaction	−0.10	−0.23–0.03	0.129	−0.10	−0.13–−0.07	<0.001
Social landscape	−0.01	−0.14–0.12	0.925	−0.03	−0.06–−0.00	0.039
SCHZ × Incongruent	−0.01	−0.03–0.02	0.595	0.01	−0.01–0.03	0.193
SCHZ × Physically salient	0.02	0.00–0.05	0.030	0.02	0.00–0.04	0.046
SCHZ × Social interaction	0.01	−0.01–0.03	0.310	0.01	−0.01–0.03	0.306
SCHZ × Social landscape	0.01	−0.02–0.03	0.532	0.02	−0.00–0.04	0.107
Random Effects						
σ^2	0.04			0.03		
τ_{00}	0.00 ID			0.00 ID		
	0.00 imageCat			0.00 imageCat		
ICC	0.06			0.05		
N	54 ID			54 ID		
	5 imageCat			5 imageCat		
Observations	13435			13097		
Marginal R^2/Conditional R^2	0.040/0.097			0.039/0.087		

sqrt square root, NSS normalised scan path, ID unique participant identification string, imageCat Image category.

Table 3. Differences in NSS scores between SCHZ a HC groups for top-down (EML-Net) model in two different time periods.

Predictors	top-down sqrt(NSS) – To the fifth fixation			top-down sqrt(NSS) – Up to sixth fixation		
	Estimates	CI	p	Estimates	CI	p
(Intercept)	1.81	1.35–2.27	<0.001	1.67	1.36–1.98	<0.001
SCHZ	−0.11	−0.17–−0.04	0.001	−0.02	−0.08–0.03	0.431
Incongruent	0.14	−0.51–0.79	0.679	0.02	−0.42–0.46	0.936
Physically salient	−0.14	−0.79–0.51	0.663	−0.13	−0.57–0.31	0.557
Social interaction	0.25	−0.40–0.90	0.443	0.20	−0.24–0.64	0.370
Social landscape	0.25	−0.40–0.89	0.460	0.05	−0.39–0.49	0.826
SCHZ × Incongruent	−0.01	−0.05–0.04	0.706	0.04	0.00–0.08	0.034
SCHZ × Physically salient	0.05	0.00–0.09	0.029	0.02	−0.01–0.06	0.232
SCHZ × Social interaction	−0.04	−0.09–−0.00	0.045	−0.08	−0.12–−0.05	<0.001
SCHZ × Social landscape	−0.05	−0.09–−0.00	0.035	0.01	−0.02–0.05	0.521
Random Effects						
σ^2	0.16			0.12		
τ_{00}	0.01 ID			0.01 ID		
	0.05 imageCat			0.02 imageCat		
ICC	0.28			0.22		
N	54 ID			54 ID		
	5 imageCat			5 imageCat		
Observations	13435			13097		
Marginal R^2/Conditional R^2	0.086/0.346			0.054/0.263		

sqrt square root, NSS normalised scan path, ID unique participant identification string, imageCat Image category.

the bottom-up model better predicted oculomotor behavior in SCHZ patients compared to HC when viewing physically salient images. This observation supports a 'bottom-up' bias in SCHZ patients and the assumption of a delayed integration of visual signals initially processed by bottom-up mechanisms into the subsequent top-down processing[26,55,56].

On the other hand, the top-down model was more effective in predicting the gaze patterns of SCHZ patients compared to HCs

Table 4. Results of psychological measurements.

Group	SCHZ				HC			
Variable	Mean of fixation number		Mean of fixation		Mean of fixation number		Mean of fixation duration	
	Pearson Correlation r(28)	p-value	Pearson Correlation r(28)	p-value	Pearson Correlation r(23)	p-value	Pearson Correlation r(23)	p-value
CPT omissions	0.12	0.52	−0.08	0.88	−0.19	0.34	0.24	0.23
CPT commissions	0.15	0.45	−0.16	0.4	−0.51	0.01	0.36	0.07
CPT hit reaction time (HRT)	−0.18	0.36	0.27	16	0.17	0.4	−0.13	0.54
CPT HRT standard deviation	−0.2	0.29	0.21	0.26	−0.26	0.21	0.05	0.86
CPT variability	−0.22	0.26	0.22	0.21	−0.24	0.23	0.13	0.53
CPT detectability	0.13	0.5	−0.09	0.64	−0.35	0.08	0.31	0.12
CPT perseverations	0.19	0.32	−0.21	0.26	0.28	0.17	−0.2	0.33
CPT HRT block change	−0.13	0.52	0.22	0.24	−0.05	0.8	−0.15	0.47
CPT HRT inter-stimulus	−0.19	0.33	0.15	0.44	−0.05	0.8	0.05	0.67
PANSS positive symptoms	−0.04	0.84	0.01	0.96	NA	NA	NA	NA
PANSS negative symptoms	−0.17	0.37	0.09	0.64	NA	NA	NA	NA
PANSS general psychopathology	−0.14	0.48	0.07	0.72	NA	NA	NA	NA
PANSS total score	−0.17	0.34	0.11	0.59	NA	NA	NA	NA
Duration of illness (months)	−0.08	0.64	0.17	0.36	NA	NA	NA	NA
Duration of untreated psychosis (months)	−0.11	0.54	0.2	0.28	NA	NA	NA	NA
CHLPMZ equivalent	−0.2	0.29	0.31	0.9	NA	NA	NA	NA

CPT Conners' Continuous Performance Test III, *PANSS* Positive and Negative Syndrome Scale, *NA* notavailable.

when they viewed incongruent scenes. This observation suggests that although the model is capable of predicting gaze patterns in relation to the objects within a scene, it falls short in recognizing the incongruity of these objects, that is, an understanding how the objects relate contextually. This observed behavior is likely because the top-down model, which inherently lacks the ability to assess the semantic context of objects, does not factor in the presence of incongruent objects within its predictive framework. In essence, the model's limited capacity to evaluate semantic contexts aligns with the similar cognitive limitation observed in SCHZ patients[63]. Therefore, the enhanced predictive accuracy of the top-down model for SCHZ patients may stem from this shared deficiency in correctly interpreting the semantic context of objects, resulting in more accurate oculomotor predictions for this group. Our findings also indicate that the top-down model more accurately predicted the oculomotor behavior of HCs compared to SCHZ patients in the context of social interactions images. This is consistent with earlier research highlighting the impaired ability of SCHZ patients to process more complex visual scenes such as social interactions and emotions[64–66]. This outcome is linked to negative symptoms of emotional blunting[67] and a deficit in processing the low spatial frequency (LSF) of images[68,69].

Category-specific stimuli analyses showed better performance in SCHZ group for the top-down model in categories of social interaction and social landscape. This finding is in agreement with previous reports on the properties of saliency models[70,71]. This enhanced prediction accuracy suggests that this model excels in accounting for higher cognitive processes associated with the interpretation of individuals and objects within the scene and their interactions. Conversely, the performance of the top-down model was less effective in predicting the oculomotor behavior of HCs in response to physically salient stimuli. The top-down model's reduced capacity to predict oculomotor behavior for physically salient stimuli reaffirms its overall lower sensitivity to the bottom-up component within the predicted saliency map.

As expected, the temporal analysis of the models allowed us to reveal how top-down and bottom-up processes are involved in cognition and its formation in the groups we studied. The bottom-up (GBVS) model indicated no significant differences between the groups across both periods. However, this trend changed when we focused on specific stimulus categories. Notably, for physically salient images, the GBVS model consistently showed better performance in SCHZ patients than in HCs during both periods. This confirms the previously reported tendency of SCHZ patients to focus their attention on physically salient stimuli[72,73]. The second analysis shows a difference in performance of the top-down (EML-Net) model between groups. Especially in the first period, the nuanced differences in how SCHZ and HC groups process visual information is highlighted. This distinction, particularly evident in the early period, underscores a potential divergence in cognitive processing strategies between the two groups. As the model's ability to differentiate between SCHZ and HC partly diminishes in the second period, it suggests a partial convergence in visual processing strategies over time, or possibly an adaptation in the SCHZ group's visual attention mechanisms. Differences persist for images depicting social interaction and emerge in incongruent images category.

Furthermore, these observations are in agreement with results from the CPT, where SCHZ patients exhibited higher rates of omission and perseveration errors compared to HCs. These CPT findings imply a greater tendency of SCHZ patients to overall inattentiveness (as indicated by higher omission scores) and to the use of more automatic responses (as evidenced by higher perseveration scores). Together, these elements suggest an impaired ability of SCHZ patients to direct their focus towards visual stimuli[74]. This impairment may also contribute to the delayed scene orientation observed in SCHZ patients, thereby

affecting the efficiency of bottom-up signal processing. In the HC population, after the initiation phase, bottom-up saliency is suppressed by the top-down saliency of higher cognitive processes[16,75–77], but as seen in the results it appears that this onset is delayed in the SCHZ population.

The delayed emergence of top-down cognitive processes is likely attributable to dysfunctions in LSF processing. LSF processing is essential for swift scene orientation, laying the groundwork for top-down predictive mechanisms and focused attention distribution within the visual scene[16]. The absence of notable differences between-groups in the second period of top-down model predictions implies that the slower initiation of top-down cognition might be linked to LSF processing abnormalities repeatedly reported in SCHZ population[61,78–80]. Previous studies mainly focus on the reduced ability of the SCHZ population to process LSFs, which has been attributed to dysfunction of the magnocellular optical pathways. However, recent findings indicate that LSFs may not be processed only by the magnocellular pathways but are likely processed in parallel in the koniocellular pathways[81,82]. Consequently, the research focus has shifted toward the retina itself in recent years[83–85]. One possible reason for the slower bottom-up signal processing in SCHZ is the inflammatory processes of retinal microvascularity, which are associated with commonly reported atrophy of retinal nerve fibers[86,87]. The outcome of this process is a low signal-to-noise ratio[88], particularly resulting in an increased level of vagueness related to the nature of a percept/signal, ultimately leading to a disruption of the decision-making process[89]. However, inflammatory processes and associated atrophy would not explain why, in early-stage and untreated first-episode patients, hypersensitivity is often encountered[55,57]. Retinal atrophy can only explain the later stages of the illness when hypersensitivity eventually progresses to hyposensitivity, which also extends to other frequencies of the visual scene[55,90,91]. An alternative explanation that would also include hypersensitivity to LSFs would be instability in retinal dopamine levels[6]. Dopamine influences the size of receptive fields, thereby affecting the sensitivity to individual frequencies of the perceived image[92]. Increased dopamine levels reduce the size of receptive fields, leading to increased sensitivity to high spatial frequencies and vice versa[93,94]. Therefore, the instability of the receptive fields may contribute significantly to the formation of the aberrant salience that is typical for schizophrenia[6].

In our study, the SCHZ patient group exhibited fewer yet longer fixations compared to the HC group, corroborating findings from existing literature[95–97]. While previous studies have suggested a link between these oculomotor differences and the severity of both negative and positive SCHZ symptoms, the nature of this association remains a subject of debate[98]. In contrast to these studies, our results did not establish a connection between the severity of SCHZ symptoms (whether negative or positive) and oculomotor behavior. This absence of correlation extended to the outcomes of the PNASS as well as to medication effects. Furthermore, we observed no significant relationship between fixation patterns and CPT performance within the SCHZ group. These findings imply that the overall ability of SCHZ patients to sustain attention does not significantly impact the results of predictive models. It raises the possibility that these specific differences in saliency and its predictive model might be considered as trait markers of SCHZ itself.

Temporal analysis of fixation duration revealed a diminishing difference between the HC and SCHZ groups over time. Initially, the SCHZ group exhibited prolonged fixations, likely indicative of extended time needed for scene orientation and LSF signal processing. However, fixation durations gradually decreased, suggesting the engagement of advanced top-down cognitive processes. This pattern aligns with the documented reduction in fixation duration and count in SCHZ during top-down cognitive tasks, such as object search or fixation within a scene[99]. This

"unknown compensatory mechanism", as the authors of the original study called it, might relate to altered receptive field sensitivity, potentially due to dopamine fluctuations in the retina and variations in retinal morphology, affecting receptive field distribution and size. However, a precise answer to this question would require more in-depth research.

In this study, we explored the application of salience models in schizophrenia (SCHZ) research, an area with limited prior investigation[100,101]. Our findings indicate that predictive models of visual saliency are potent tools for identifying errors in visual information processing and the development of aberrant saliency in SCHZ patients. Emphasis should be placed on incongruent stimuli, stimuli that are physically salient, and complex stimuli depicting social interactions. These types of stimuli effectively illustrate the limitations of the models and the specific abnormalities in visual processing among the SCHZ population. Our study also reveals that the previously documented bias in SCHZ patients towards bottom-up signals[31,55,57,61,102,103] is variable over time, possibly originating from disruptions in early-stage visual processing. This disruption might further impede the onset of top-down visual cognition. The altered and prolonged processing of bottom-up signals likely leads to flawed and unstable internal representations of the world, impacting higher cognitive functions[6]. Our study highlights the complex interaction between bottom-up and top-down processes in the visual signal processing of SCHZ patients, marked by a progressive decrease in fixation duration. However, to fully comprehend these intricate dynamics, further research is essential.

Limitations
The first limitation of the presented study arises from the above-mentioned question: to what extent the presented saliency models reflect purely "bottom-up" and "top-down" processing? Although this is still a matter of debate, the proportion of these two components largely differs in the applied models and thus the presented methodology can describe the differences between HC and SCHZ bottom-up and top-down processing. Also, the top-down EML-Net model, having been trained on data from individuals without neurological conditions, presents a challenge in interpretation: it's unclear whether the improved model fit observed in the control group is due to differences in the type of top-down information prioritized by patients and controls, or if it simply reflects variances in the degree to which they prioritize such information. This ambiguity raises questions about the model's ability to accurately capture the nuances of top-down information processing in populations with neurological conditions like SCHZ. Other limitation pertains to the antipsychotic treatment of SCHZ participants. The relationship between antipsychotic medication and oculomotor movement is a controversial topic which has been questioned before[104–106], and our results support these concerns.

METHODS
Participants
This study involved 62 subjects (37 SCHZ and 25 HC) (Table 5), matched in age, sex, and years of education (within ± 2 years). Some HCs were matched to a larger number of SCHZ patients due to the lower availability of HCs with fewer years of education, resulting in this imbalance. The number of participants was estimated by a power analysis (Appendix A). Nine participants (9 SCHZ, 0 HC) were excluded due to incorrect eye-tracking measurements (within the measurement, the calibration deviation increased to more than 0.5°; high blink rate; fatigue; and concentration problems). Participants were recruited into the study as part of the Early-Stage Schizophrenia Outcome (ESO) Study[107–109] and through the National Institute of Mental Health

clic, Czech Republic (NIMH CZ). The diagnostic procedure was standardized with the structured Mini-International Neuropsychiatric Interview[110], and patients were diagnosed according to ICD-10[111]. Only patients diagnosed with schizophrenia spectrum disorder were included in the analyses (i.e., F20, F23 and F25)[111]. Additional inclusion criteria were age between 18 and 60 years, the absence of severe neurological illness or organic brain problems, and normal color vision as determined by the Ishihara test[112]. All the patients took medication at the time of participation. HCs were recruited via an advertisement from a similar socio-demographic background to the SCHZ participants.

HCs were not allowed to have a history of psychiatric disorders (evaluated with a modified version of the M.I.N.I.) or in their first- and second-degree family members (assessed by an anamnestic questionnaire). Both groups were recruited between 2018 and 2021. The ethics committee of the NIMH CZ approved the study. All the experiments were performed in accordance with the relevant guidelines and regulations. Written, informed consent was obtained from all the subjects after receiving a complete study description. Participation in the research was voluntary, with a financial compensation of 500 CZK. In the SCHZ group, the current clinical condition and medication dose were also taken into consideration.

Table 5. Demographic and clinical characteristics of the experimental groups.

Variable	SCHZ (n = 30) Mean (SD)	HC (n = 25) Mean (SD)	p-value
Gender (F/M)	10/20	10/15	0.817
Age (years)	32 (9.1)	31.57 (7.57)	0.837
Education (years)	14.11 (2.64)	14.28 (2.15)	0.777
PANSS total score	37.6 (7.43)		
PANSS positive symptoms	8.18 (1.1)		
PANSS negative symptoms	11.06 (4.7)		
PANSS general symptoms	18.53 (3.03)		
CPT omissions	55.43 (14.84)	47.15 (4.63)	0.017
CPT perseverations	54.84 (11.55)	48.61 (7.81)	0.015
CPT commissions	54.62 (9.72)	53.15 (10.99)	0.583
CHLPMZ equivalent	399.1 (182.14)		
Duration of untreated psychosis (months)	5.12 (8.03)		
Duration of illness (months)	133.72 (170.45)		
Ratio of individual SCHZ diagnoses	F20 (n = 20); F23 (n = 10); F25 (n = 0)		

CHLPMZ Chlorpromazine.

Visual stimuli selection and pre-processing

A total of 250 color images of an everyday naturalistic scene were used in the study. All the photographs were downloaded from public databases (Flicker, World Images, and Vecteezy) or taken by the study's authors. The stimuli were divided into five categories (50 images pear each), based on their content (congruent, incongruent, physically salient, social landscape, social interaction) (Fig. 3). (1) Everyday Scenes (Congruent): This category includes images of typical, everyday environments where all elements are contextually appropriate and consistent. Such congruent scenes are expected to align well with top-down models' predictions, as they match usual expectations of everyday environments. (2) Incongruent images: These scenes contain everyday settings but with objects that are contextually out of place or unusual. The incongruence of these objects is anticipated to challenge top-down models, which rely on contextual appropriateness, and could be more accurately predicted for individuals with SCHZ than HC due to the expected bottom-up bias in SCHZ[56]. (3) Natural Scenes with Physically Salient Elements: Scenes in this category are natural environments that include elements with notable physical salience—like unusual color, contrast, or orientation. These elements are expected to be more effectively predicted by bottom-up models, and thus potentially better predicted for individuals in the SCHZ group. (4) Scenes Depicting Social Interactions: This category comprises scenes focused on social interactions. These types of stimuli are expected to be more accurately predicted by top-down model for the HC group, as they involve understanding social cues and contexts. 5) Social Landscapes: These are natural scenes that include elements of nature and feature humans. Termed "social landscapes," these scenes are anticipated to align better with top-down model predictions for

Fig. 3 Examples of stimuli utilized in the experiment. The photographs were categorized into five different groups based on their content. (1) Everyday Scenes (Congruent) include images of typical, everyday environments where all elements are contextually appropriate and consistent. (2) Incongruent images contain everyday scenes but with objects that are contextually out of place or unusual. (3) Natural Scenes with Physically Salient Elements include natural environments that include elements with notable physical salience. (4) Scenes Depicting Social Interactions comprises scenes depicting social interactions. (5) Social Landscapes are natural scenes that include elements of nature, but feature also humans.

the HC group, as they combine elements of nature with social interactions.

The Shine toolbox[113] for MATLAB was used to normalize all the stimuli to color and luminance. Then two saliency models, Expandable Multi-Layer NETwork (EML-Net) and Graph-Based Visual Saliency Model (GBVS) (See below in section 4.6), were applied to each photograph, producing one saliency map per image and model. Subsequently, a black border was added to each image to reach a resolution of 3840 × 2160 pixels. The original mean image area was $M = 6,029,277.12$ pix, SD = 818,762.31. The mean area of the added black borders was $M = 1,487,522.88$ pix, SD = 818,762.31. The image area therefore occupied approximately 80% of the monitor area. The experiment was created and presented using SR Research Experiment Builder 2.3.1[114].

Eye-tracking data acquisition
Eye movements were recorded using the EyeLink 1000 Plus eye tracker (SR Research Ltd. Ottawa, Ontario, Canada). The eye-tracker samples raw gaze data at 1000 Hz, fixations and saccadic movements are derived from that. Stimuli images were presented on a 4 K 27″ (3840 × 2160, 163 PPI, 60 Hz refresh rate) IPS screen with 100% sRGB color space. The screen was color- and luminance-calibrated with X-Rite i1 Display Pro probes connected during the whole rating session to adjust the screen for ambient light. The eye tracking and rating session took place in a quiet and windowless eye tracking lab in standardized conditions across all raters. Raters were seated with their heads on a chin and forehead rest (SR Research Head Support) 70 cm from the screen. Every participant saw images in a randomized order, with instructions to freely observe image on the computer screen.

We determined the dominant eye of each participant using a variation of the Porta test[115]. Although vision is binocular, we tracked only the dominant eye. The eye tracker was calibrated by a standard nine-point routine. Calibrations was validated by the EyeLink software and repeated as necessary until the optimal calibration criterion is reached.

Each image begun with a drift correction. A fixation cross on an 18% grey background appeared (in eight possible positions) on the screen, and participants were instructed to focus their gaze on it. The distance of the centers of the corner crosses from the center of image was 1275 pix at angles of 155°; −155°; 25°; −25°. The centers of the crosses above and below the image center were 542 pix at angles of 90° and −90°. The centers of the crosses to the right and left of the image center were 1150 pix at the angles of 0° and 180°. The cross size was 183 pix with a stroke thickness of 7 pix. The semi-random position of the cross out of the center was chosen to avoid visual bias towards the center of the image. When a participant's eye fixates on the cross, the stimuli presentation will initiate for five seconds.

Symptom rating and cognitive testing
After conducting the eye-tracking measurements, we utilized the Positive and Negative Syndrome Scale (PANSS)[116] to assess the severity of positive and negative symptoms in SCHZ patients. Additionally, we employed Conners' Continuous Performance Test III (CPT)[117] to evaluate attention. We hypothesized that diminished attention, as indicated by the CPT, would influence perception processing, given that visual attention is crucial for acquiring information visually[117]. These assessments were conducted at the National Institute of Mental Health (NIMH CZ) in a quiet, dedicated room. The entire assessment process, led by a trained psychologist, lasted approximately 2 hours. The primary objective of this psychological testing was to investigate any potential causal links between the illness, the performance of the saliency models, and the oculomotor behavior observed in the patients.

Data pre-processing and statistics
Primary pre-processing (differentiation between saccades and fixations) was performed in the EyeLink Data Viewer. The data were then exported to a spreadsheet format (CSV) for further processing. In the first step, all ET data were cleaned of off-monitor fixations and saccades. The first fixation overlapping with the fixation cross between stimuli was removed and no longer considered. Pre-processing and all table data (including PANSS, CPT, saliency prediction scores, and demographic data) were statistically analyzed with R[118] using the tidyverse package[119].

Ground truth fixation matrices were calculated from the cleaned fixation data for each participant and image in Python using the GazePointHeatMap package[120]. This matrix contains the fixation averages for each image area over time. Ground truth fixation map was in full resolution of the original stimuli (3840 × 2160). Two subsequent ground truth maps from fixations were computed (up to the fifth fixation and from the sixth fixation) to examine whether the bottom-up signal bias in the SCHZ group persists over time or not. Python was used to process both saliency models, which are published at github.com (GBVS[121]; EML-Net[122]). The final performance evaluation of each saliency model was calculated using the MIT saliency benchmark toolbox[40] in MATLAB (Fig. 4).

The inter-group difference in the total examined image area was calculated using the standard distance deviation formula (SDD) in R with the mapTool package[123]. We investigated the relationship between the oculomotor behavior of SCHZ patients and key clinical factors: the duration of untreated psychosis and the chlorpromazine equivalent[54,124,125] were investigated in R.

Finally, the metrics differences between-groups were evaluated using Linear Mixed-Effects Models (R lme4 package)[126]. The models used NSS metrics value as the dependent variable and included fixed effects for interaction between-group (patients vs controls), image category, crossed random intercepts for each individual (participants ID) and each image category. Estimating random intercepts for individual images was not feasible due to the extensive number of parameters required. Prior to modelling, the NSS score was transformed using square root transformation to suppress skewness of the distribution. Inputs and resulting distributions, as well as model residuals, were checked using density and q-q plots. Significance tests on fixed effects were performed using Satterthwaite's method (R lmerTest package)[127].

The Wilcoxon signed-rank test was applied to assess saccadic eye movement, which had a non-normal distribution. A Pearson's correlation test was used to assess the association between medication, the outcomes of psychological tests, and the duration of untreated psychosis with the findings of the oculomotor movements. For all the tests, the significance level was set at alpha < 0.001 in order to take into consideration multiple comparisons.

For the between-group comparison of fixation duration, we used the sequential testing procedure: starting from fixation 1, the between-group differences were compared using the t-test at a significance level alpha = 0.05. The subsequent fixations were considered significant if, and only if, current and all preceding tests rejected the null hypothesis. This approach conforms to the closed testing procedure and thus controls the overall significance level at alpha = 0.05[128].

Saliency Models
The selection of the most recent top-down and bottom-up saliency models used in our study was based on the models' overall success in their category as measured by the MIT Saliency Benchmark (saliency.mit.edu)[40]. We selected the best-performing models from the top-down and bottom-up categories based on the NSS metrics[129–132], which was set as a mandatory performance indicator at the 14th European Conference on Computer Vision[40]. The second criterion was the availability of source code. We chose the results from a MIT300 dataset[131], which by its nature, better
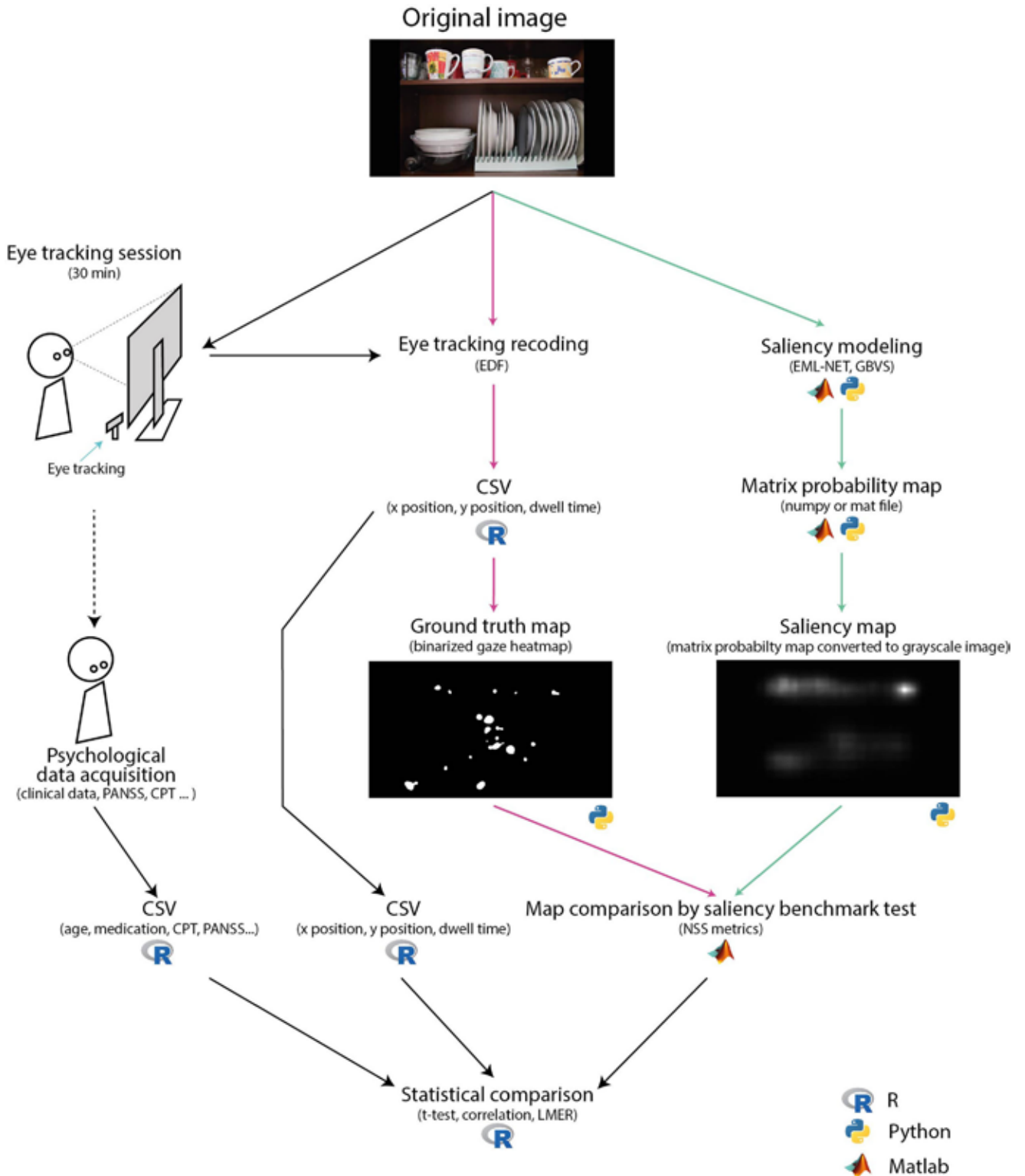
Fig. 4 The diagram illustrating data processing and analysis steps utilized in the study. Pink arrows mark the processing path of the ground truth map. Green arrows mark the processing path of the saliency models. Black arrows mark the processing path of table data for statistical comparison; CSV comma-separated values, EDF standardized European data format for storage of medical time series, NSS normalized scan path saliency, PANSS Positive and Negative Syndrome Scale, CPT Conners' Continuous Performance Test III.

reflects the stimuli used in our study than a CAT2000[133], which contains only natural scenery.

As the bottom-up model, we selected the pre-trained GBVS[134], which works by constructing a graph representation of the image, where each node in the graph corresponds to a small region of the image. This process consists of two steps. First, it creates numerical activation maps of feature channels extracted from locations in the image (e.g., by linear filtering followed by

elementary nonlinear filtering). Second, it normalizes the activation maps in a way that emphasizes conspicuity and allows combinations with other maps[135]. The model takes a Markovian approach at both steps. Markov chains are defined over various image maps, and the equilibrium distribution over map locations is treated as activation and saliency values. The edges between the nodes represent the similarity between the regions. The model then computes a saliency value for each node based on its contrast with neighboring regions. The nodes with high saliency values are considered to be the most visually salient regions of the image and are likely to attract human attention.

As the top-down model, we selected the pre-trained EML-Net[136], a deep-learning model used for image saliency prediction. The EML-Net model uses CNN layers to extract features from the image and then passes these features through multiple layers of fully connected neural network layers to predict the saliency. Specifically, the encoder consists of NasNet from ImageNet and DenseNet from PLACE365[136], both are used as encoder for image classification. During training, the model learns to predict the saliency map for a given input image by adjusting the weights of the neurons in the network to minimize the difference between the predicted saliency map and the ground truth map.

To enable a meaningful comparison between two distinct prediction models, the NSS metrics were selected to evaluate their performance[40]. Specifically, NSS metrics measure accuracy by comparing the predicted saliency map created by the model with the fixation density map from eye-tracking data (ground truth map).[129] The fixation density map shows where viewers look at an image. NSS calculates the mean saliency value at the fixated locations by comparing the predicted map with a binary fixation map, where 'ones' represent fixations and 'zeros' represent other areas[137]. A higher NSS value suggests a better prediction of viewer attention, while a value of zero indicates chance-level predictions. NSS is widely used for comparing different saliency models because it provides a straightforward and standardized way to assess their performance.

DATA AVAILABILITY

The data analyzed during the current study are available from the corresponding author upon reasonable request. Analysis scripts are available on the OSF: https://osf.io/hz2p8/.

REFERENCES

1. Kalkstein, S., Hurford, I. & Gur, R. C. Neurocognition in schizophrenia. *Behavioral neurobiology of schizophrenia and its treatment*. (ed. Swerdlow, N.) Current Topics in Behavioral Neurosciences, Vol. 4 (Springer, Berlin, Heidelberg, 2010). https://doi.org/10.1007/7854_2010_42.
2. Yan, Y., Zhaoping, L. & Li, W. Bottom-up saliency and top-down learning in the primary visual cortex of monkeys. *Proc. Natl Acad. Sci.* **115**, 10499–10504 (2018).
3. Melloni, L., van Leeuwen, S., Alink, A. & Müller, N. G. Interaction between bottom-up saliency and top-down control: how saliency maps are created in the human brain. *Cerebral cortex* **22**, 2943–2952 (2012).
4. Chun, C. A., Brugger, P. & Kwapil, T. R. Aberrant salience across levels of processing in positive and negative schizotypy. *Front. Psychol.* **10**, 2073 (2019).
5. Kapur, S. Psychosis as a state of aberrant salience: a framework linking biology, phenomenology, and pharmacology in schizophrenia. *Am. J. Psychiatry* **160**, 13–23 (2003).
6. Adámek, P., Langová, V. & Horáček, J. Early-stage visual perception impairment in schizophrenia, bottom-up and back again. *Schizophrenia* **8**, 1–12 (2022).
7. Stokes, D. & Biggs, S. The dominance of the visual. *Perception and its Modalities*, 350–378 (2014).
8. Hirst, R. J., Cragg, L. & Allen, H. A. Vision dominates audition in adults but not children: A meta-analysis of the Colavita effect. *Neurosci. Biobehav. Rev.* **94**, 286–301 (2018).
9. Levin, L. A. et al. *Adler's Physiology of the Eye E-Book: Expert Consult-Online and Print*. (Elsevier Health Sciences, 2011).
10. Sziklai, G. Some studies in the speed of visual perception. *IRE Trans. Inf. Theory* **2**, 125–128 (1956).
11. Carrasco, M. Visual attention: The past 25 years. *Vis. Res.* **51**, 1484–1525 (2011).
12. Wässle, H. Parallel processing in the mammalian retina. *Nat. Rev. Neurosci.* **5**, 747–757 (2004).
13. Kamkar, S., Moghaddam, H. A. & Lashgari, R. Early visual processing of feature saliency tasks: a review of psychophysical experiments. *Front. Syst. Neurosci.* **12**, 54 (2018).
14. Ungerleider, S. K. & G, L. Mechanisms of visual attention in the human cortex. *Ann. Re. Neurosci.* **23**, 315–341 (2000).
15. Rauss, K., Schwartz, S. & Pourtois, G. Top-down effects on early visual processing in humans: A predictive coding framework. *Neurosci. Biobehav. Rev.* **35**, 1237–1253 (2011).
16. Panichello, M. F., Cheung, O. S. & Bar, M. Predictive feedback and conscious visual experience. *Front. Psychol.* **3**, 620 (2013).
17. Bar, M. et al. Top-down facilitation of visual recognition. *Proc. Natl Acad. Sci.* **103**, 449–454 (2006).
18. Gordon, N., Tsuchiya, N., Koenig-Robert, R. & Hohwy, J. Expectation and attention increase the integration of top-down and bottom-up signals in perception through different pathways. *PLoS Biol.* **17**, e3000233 (2019).
19. Kauffmann, L., Ramanoël, S. & Peyrin, C. The neural bases of spatial frequency processing during scene perception. *Frontiers in Integr. Neurosci.* **8**, 37 (2014).
20. Parr, T. & Friston, K. J. Attention or salience? *Curr. Opin. Psychol.* **29**, 1–5 (2019).
21. Roiser, J. et al. Do patients with schizophrenia exhibit aberrant salience? *Psychol. Med.* **39**, 199–209 (2009).
22. Butler, P. D. et al. Dysfunction of early-stage visual processing in schizophrenia. *Am. J. Psychiatry* **158**, 1126–1133 (2001).
23. Butler, P. D. et al. Early-stage visual processing and cortical amplification deficits in schizophrenia. *Archives Gen. Psychiatry* **62**, 495–504 (2005).
24. Martínez, A. et al. Magnocellular pathway impairment in schizophrenia: evidence from functional magnetic resonance imaging. *J. Neurosci.* **28**, 7492–7500 (2008).
25. Silverstein, S. M. et al. An fMRI examination of visual integration in schizophrenia. *J. Integr. Neurosci.* **8**, 175–202 (2009).
26. Butler, P. D., Silverstein, S. M. & Dakin, S. C. Visual perception and its impairment in schizophrenia. *Biol. Psychiatry* **64**, 40–47 (2008).
27. Clark, C. M., Gosselin, F. & Goghari, V. M. Aberrant patterns of visual facial information usage in schizophrenia. *Ann. Rev. Clin. Psychol.* **122**, 513 (2013).
28. Sehatpour, P. et al. Impaired visual object processing across an occipital-frontal-hippocampal brain network in schizophrenia: an integrated neuroimaging study. *Archives Gen. Psychiatry* **67**, 772–782 (2010).
29. Silverstein, S. et al. Reduced top-down influences in contour detection in schizophrenia. *Cogn. Neuropsychiatry* **11**, 112–132 (2006).
30. Uhlhaas, P. J., Phillips, W. A., Mitchell, G. & Silverstein, S. M. Perceptual grouping in disorganized schizophrenia. *Psychiatry Res.* **145**, 105–117 (2006).
31. Dima, D., Dietrich, D. E., Dillo, W. & Emrich, H. M. Impaired top-down processes in schizophrenia: a DCM study of ERPs. *Neuroimage* **52**, 824–832 (2010).
32. King, D. J., Hodgekins, J., Chouinard, P. A., Chouinard, V.-A. & Sperandio, I. A review of abnormalities in the perception of visual illusions in schizophrenia. *Psychonomic Bull. Rev.* **24**, 734–751 (2017).
33. Notredame, C.-E., Pins, D., Deneve, S. & Jardri, R. What visual illusions teach us about schizophrenia. *Front. Integr. Neurosci.* **8**, 63 (2014).
34. Yang, E. et al. Visual context processing in schizophrenia. *Clin. Psychol. Sci.* **1**, 5–15 (2013).
35. Doniger, G. M., Silipo, G., Rabinowicz, E. F., Snodgrass, J. G. & Javitt, D. C. Impaired sensory processing as a basis for object-recognition deficits in schizophrenia. *Am. J. Psychiatry* **158**, 1818–1826 (2001).
36. Butler, P. D. et al. An event-related potential examination of contour integration deficits in schizophrenia. *Front. Psychol.* **4**, 132 (2013).
37. Luck, S. J., Leonard, C. J., Hahn, B. & Gold, J. M. Is attentional filtering impaired in schizophrenia? *Schizophr. Bull.* **45**, 1001–1011 (2019).
38. Wichowicz, H. M., Ciszewski, S., Żuk, K. & Rybak-Korneluk, A. Hollow mask illusion–is it really a test for schizophrenia. *Psychiatr. Pol* **50**, 741–745 (2016).
39. Christensen, B. K., Spencer, J. M., King, J. P., Sekuler, A. B. & Bennett, P. J. Noise as a mechanism of anomalous face processing among persons with Schizophrenia. *Front. Psychol.* **4**, 401 (2013).
40. Bylinskii, Z. et al. A. Mit saliency benchmark, 13 (2015).
41. Hayes, T. R. & Henderson, J. M. Deep saliency models learn low-, mid-, and high-level features to predict scene attention. *Sci. Rep.* **11**, 1–13 (2021).
42. Itti, L. & Koch, C. Computational modelling of visual attention. *Nat. Rev. Neurosci.* **2**, 194–203 (2001).
43. Koch, C. & Ullman, S. Shifts in selective visual attention: towards the underlying neural circuitry. *Hum. Neurobiol.* **4**, 219–227 (1985).

44. Itti, L., Koch, C. & Niebur, E. A model of saliency-based visual attention for rapid scene analysis. *IEEE Trans. Pattern Anal. Mach. Intell.* **20**, 1254–1259 (1998).

45. Veale, R., Hafed, Z. M. & Yoshida, M. How is visual salience computed in the brain? Insights from behaviour, neurobiology and modelling. *Philos. Trans. Royal Soc. B: Biol. Sci.* **372**, 20160113 (2017).

46. Torralba, A., Oliva, A., Castelhano, M. S. & Henderson, J. M. Contextual guidance of eye movements and attention in real-world scenes: the role of global features in object search. *Psychol. Rev.* **113**, 766 (2006).

47. Bogler, C., Bode, S. & Haynes, J.-D. Decoding successive computational stages of saliency processing. *Curr. Biol.* **21**, 1667–1671 (2011).

48. Chen, T., Lin, L., Liu, L., Luo, X. & Li, X. DISC: Deep image saliency computing via progressive representation learning. *IEEE Trans. Neural Netw. Learn. Syst.* **27**, 1135–1149 (2016).

49. Murabito, F. et al. Top-down saliency detection driven by visual classification. *Comput. Vis. Image Understand.* **172**, 67–76 (2018).

50. Pan, J., Sayrol, E., Giro-i-Nieto, X., McGuinness, K. & O'Connor, N. E. in *Proceedings of the IEEE Conference On Computer Vision And Pattern Recognition*. 598–606.

51. Zhu, G., Wang, Q. & Yuan, Y. Tag-saliency: Combining bottom-up and top-down information for saliency detection. *Comput. Vis. Image Understand.* **118**, 40–49 (2014).

52. Borji, A. In i*eee* conf*erence on computer vision and pattern recognition*. 438-445 (IEEE) (2012).

53. Mahdi, A., Qin, J. & Crosby, G. DeepFeat: A bottom-up and top-down saliency model based on deep features of convolutional neural networks. *IEEE Trans. Cogn. Dev. Syst.* **12**, 54–63 (2019).

54. Bansal, S. et al. Failures in top-down control in schizophrenia revealed by patterns of saccadic eye movements. *Ann. Rev. Clin. Psychol.* **128**, 415 (2019).

55. Silverstein, S. M. Visual Perception Disturbances in Schizophrenia: A Unified Model. In: *The Neuropsychopathology of Schizophrenia. Nebraska Symposium on Motivation*, Vol. 63 (eds Li, M, & Spaulding, W.) (Springer, Cham, 2016). https://doi.org/10.1007/978-3-319-30596-7_4.

56. Javitt, D. C. When doors of perception close: bottom-up models of disrupted cognition in schizophrenia. *Ann. Rev. Clin. Psychol.* **5**, 249–275 (2009).

57. Born, R. T. & Bencomo, G. M. Illusions, delusions, and your backwards Bayesian brain: A biased visual perspective. *Brain Behav. Evol.* **95**, 272–285 (2020).

58. Gao, W.-J., Yang, S.-S., Mack, N. R. & Chamberlin, L. A. Aberrant maturation and connectivity of prefrontal cortex in schizophrenia—contribution of NMDA receptor development and hypofunction. *Mol. Psychiatry* **27**, 731–743 (2022).

59. Li, S. et al. Dysconnectivity of multiple brain networks in schizophrenia: a meta-analysis of resting-state functional connectivity. *Front. Psychiatry* **10**, 482 (2019).

60. Wheeler, A. L. & Voineskos, A. N. A review of structural neuroimaging in schizophrenia: from connectivity to connectomics. *Front. Hum. Neurosci.* **8**, 653 (2014).

61. Laprevote, V. et al. Low spatial frequency bias in schizophrenia is not face specific: when the integration of coarse and fine information fails. *Front. Psychol.* **4**, 248 (2013).

62. Schütt, H. H., Rothkegel, L. O., Trukenbrod, H. A., Engbert, R. & Wichmann, F. A. Disentangling bottom-up versus top-down and low-level versus high-level influences on eye movements over time. *Journal of vision* **19**, 1–1 (2019).

63. Tschacher, W., Genner, R., Bryjová, J., Schaller, E. & Samson, A. C. Investigating vision in schizophrenia through responses to humorous stimuli. *Schizophr. Res.: Cogn.* **2**, 84–88 (2015).

64. Li, X.-B. et al. The attenuated visual scanpaths of patients with schizophrenia whilst recognizing emotional facial expressions are worsened in natural social scenes. *Schizophr. Res.* **220**, 155–163 (2020).

65. Matsumoto, Y., Takahashi, H., Murai, T. & Takahashi, H. Visual processing and social cognition in schizophrenia: relationships among eye movements, biological motion perception, and empathy. *Neurosci. Res.* **90**, 95–100 (2015).

66. Asgharpour, M., Tehrani-Doost, M., Ahmadi, M. & Moshki, H. Visual attention to emotional face in schizophrenia: an eye tracking study. *Iran. J. Psychiatry* **10**, 13 (2015).

67. Gao, Z. et al. Facial emotion recognition in schizophrenia. *Front. Psychiatry* **12**, 633717 (2021).

68. Marosi, C., Fodor, Z. & Csukly, G. From basic perception deficits to facial affect recognition impairments in schizophrenia. *Sci. Rep.* **9**, 8958 (2019).

69. Obayashi, C. et al. Decreased spatial frequency sensitivities for processing faces in male patients with chronic schizophrenia. *Clin. Neurophysiol.* **120**, 1525–1533 (2009).

70. Zhang, D. & Zakir, A. Top–down saliency detection based on deep-learned features. *Int. J. Comput. Intell. Appl.* **18**, 1950009 (2019).

71. Krasovskaya, S. & MacInnes, W. J. Salience models: A computational cognitive neuroscience review. *Vision* **3**, 56 (2019).

72. Hahn, B. et al. Failure of schizophrenia patients to overcome salient distractors during working memory encoding. *Biol. Psychiatry* **68**, 603–609 (2010).

73. Kornmayer, L., Leicht, G. & Mulert, C. Attentional capture by physically salient stimuli in the gamma frequency is associated with schizophrenia symptoms. *World J. Biol. Psychiatry* **19**, S52–S62 (2018).

74. Sklar, A. L. et al. Inefficient visual search strategies in the first-episode schizophrenia spectrum. *Schizophr. Res.* **224**, 126–132 (2020).

75. Trapp, S. & Bar, M. Prediction, context, and competition in visual recognition. *Ann. New York Acad. Sci.* **1339**, 190–198 (2015).

76. De Lange, F. P., Heilbron, M. & Kok, P. How do expectations shape perception? *Trends Cogn. Sci.* **22**, 764–779 (2018).

77. Theeuwes, J. Top–down and bottom–up control of visual selection. *Acta Psychol.* **135**, 77–99 (2010).

78. Calderone, D. J. et al. Contributions of low and high spatial frequency processing to impaired object recognition circuitry in schizophrenia. *Cerebr. Cortex* **23**, 1849–1858 (2013).

79. Shoshina, I., Shelepin, Y., Vershinina, E. & Novikova, K. The spatial-frequency characteristics of the visual system in schizophrenia. *Hum. Physiol.* **41**, 251–260 (2015).

80. Zemon, V. et al. Contrast sensitivity deficits in schizophrenia: A psychophysical investigation. *Euro. J. Neurosci.* **53**, 1155–1170 (2021).

81. Masri, R. A., Grünert, U. & Martin, P. R. Analysis of parvocellular and magnocellular visual pathways in human retina. *J. Neurosci.* **40**, 8132–8148 (2020).

82. Solomon, S. G. In *Handbook of clinical neurology* 178 31–50 (Elsevier, 2021).

83. Lee, W. W., Tajunisah, I., Sharmilla, K., Peyman, M. & Subrayan, V. Retinal nerve fiber layer structure abnormalities in schizophrenia and its relationship to disease state: evidence from optical coherence tomography. *Investig. Ophthalmol. Vis. Sci.* **54**, 7785–7792 (2013).

84. Gracitelli, C. P. et al. Ophthalmology issues in schizophrenia. *Curr. Psychiatry Rep.* **17**, 1–11 (2015).

85. Jurišić, D. et al. New insights into schizophrenia: a look at the eye and related structures. *Psychiatria Danubina* **32**, 60–69 (2020).

86. Jurišić, D., Ćavar, I., Sesar, A., Sesar, I., Vukojević, J., & Ćurković, M. New Insights into Schizophrenia: a Look at the Eye and Related Structures. *Psychiatr Danub.* **32**, 60–69 (2020).

87. Hanson, D. R. & Gottesman, I. I. Theories of schizophrenia: a genetic-inflammatory-vascular synthesis. *BMC Med. Genet.* **6**, 1–17 (2005).

88. de Lecea, L., Carter, M. E. & Adamantidis, A. Shining light on wakefulness and arousal. *Biol. Psychiatry* **71**, 1046–1052 (2012).

89. Shoshina, I. et al. The internal noise of the visual system and cognitive functions in schizophrenia. *Procedia Comput. Sci.* **169**, 813–820 (2020).

90. Skottun, B. C. & Skoyles, J. R. Contrast sensitivity and magnocellular functioning in schizophrenia. *Vis. Res.* **47**, 2923–2933 (2007).

91. Born, R. T. & Bencomo, G. M. Illusions, delusions, and your backwards bayesian brain: a biased visual perspective. *Brain Behav. Evol.* **95**, 272–285 (2021).

92. Scheir, G., Hanselaer, P. & Ryckaert, W. Pupillary light reflex, receptive field mechanism and correction for retinal position for the assessment of visual discomfort. *Lighting Res. Technol.* **51**, 291–303 (2019).

93. Zhang, A. J., Jacoby, R. & Wu, S. M. Light-and dopamine-regulated receptive field plasticity in primate horizontal cells. *J. Compar. Neurol.* **519**, 2125–2134 (2011).

94. K. Y. Wong et al. 26, 808 (Elsevier Health Science, 2011).

95. Bestelmeyer, P. E. G. et al. Global visual scanning abnormalities in schizophrenia and bipolar disorder. *Schizophr. Res.* **87**, 212–222 (2006).

96. Takahashi, S. et al. Impairment of exploratory eye movement in schizophrenia patients and their siblings. *Psychiat. Clin. Neurosci.* **62**, 487–493 (2008).

97. Loughland, C. M., Williams, L. M. & Harris, A. W. Visual scanpath dysfunction in first-degree relatives of schizophrenia probands: evidence for a vulnerability marker? *Schizophr Res* **67**, 11–21 (2004).

98. Beedie, S. A., Clair, D. M. S. & Benson, P. J. Atypical scanpaths in schizophrenia: evidence of a trait-or state-dependent phenomenon? *J. Psychiatry Neurosci.* **36**, 150–164 (2011).

99. Dowiasch, S. et al. Eye movements of patients with schizophrenia in a natural environment. *Eur. Arch. Psychiatry Clin. Neurosci.* **266**, 43–54 (2016).

100. Polec, J. et al. In *2017 I*EEE 11th *International Conference on Application of Information and Communication Technologies (AICT)*. 1-5 (IEEE).

101. Yoshida, M. et al. Aberrant visual salience in participants with schizophrenia during free-viewing of natural images. *medRxiv*, 2022.2011.2021.22282553 (2022). https://doi.org/10.1101/2022.11.21.22282553

102. Barnes, C. et al. F78. Overcoming a bottom-up attentional bias by providing top-down information during working memory encoding in schizophrenia. *Schizophr. Bull.* **44**, S250 (2018).

103. Dima, D. et al. Understanding why patients with schizophrenia do not perceive the hollow-mask illusion using dynamic causal modelling. *Neuroimage* **46**, 1180–1186 (2009).

104. Morita, K. et al. Eye movement abnormalities and their association with cognitive impairments in schizophrenia. *Schizophr. Res.* **209**, 255–262 (2019).

105. Beedie, S. A., Benson, P. J., Giegling, I., Rujescu, D. & St Clair, D. M. Smooth pursuit and visual scanpaths: independence of two candidate oculomotor risk markers for schizophrenia. *World J. Biol. Psychiatry* **13**, 200–210 (2012).
106. Hori, Y., Fukuzako, H., Sugimoto, Y. & Takigawa, M. Eye movements during the Rorschach test in schizophrenia. *Psychiat Clin. Neurosci.* **56**, 409–418 (2002).
107. McWhinney, S. et al. Obesity as a risk factor for accelerated brain ageing in first-episode psychosis—a longitudinal study. *Schizophr. Bull.* **47**, 1772–1781 (2021).
108. Melicher, T. et al. White matter changes in first episode psychosis and their relation to the size of sample studied: a DTI study. *Schizophr. Res.* **162**, 22–28 (2015).
109. Mikolas, P. et al. Connectivity of the anterior insula differentiates participants with first-episode schizophrenia spectrum disorders from controls: a machine-learning study. *Psychol. Med.* **46**, 2695–2704 (2016).
110. Sheehan, D. V. et al. The Mini-International Neuropsychiatric Interview (MINI): the development and validation of a structured diagnostic psychiatric interview for DSM-IV and ICD-10. *J. Clin. Psychiatry* **59**, 22–33 (1998).
111. Organization, W. H. ICD-10. International Statistical Classification of Diseases and Related Health Problems: Tenth Revision 1992, Volume 1= CIM-10. *Classification statistique internationale des maladies et des problèmes de santé connexes: Dix-ième Révision 1992*, 1, 32–6 (1992).
112. Clark, J. H. The Ishihara test for color blindness. *Am. J. Physiol. Opt.* **5**, 269–276 (1924).
113. *SHINE_color and Lum_fun: A set of tools to control luminance of colorful images v.* 0.3 (2021).
114. S. R. Research *Experiment Builder v. 2.3.1* (SR Research Ltd., Mississauga, Ontario, Canada, 2020).
115. Crovitz, H. F. & Zener, K. A group-test for assessing hand-and eye-dominance. *Am. J. Psychol.* **75**, 271–276 (1962).
116. Kay, S. R., Opler, L. A. & Lindenmayer, J.-P. The positive and negative syndrome scale (PANSS): rationale and standardisation. *Br. J. Psychiatry* **155**, 59–65 (1989).
117. Conners, K. C. & Staff, M. *Conners' Continuous Performance Test II. CPT II*. (Multi-Health Systems North Tonawanda, NY, 2004).
118. R: A language and environment for statistical computing. *R Found. Stat. Comput. v. 4.2.1* (2020).
119. Wickham, H. et al. Welcome to the Tidyverse. *J. Open Source Softw*. **4**, 1686 (2019).
120. Roeddiger, T. GazePointHeatMap. Retrieved from https://github.com/TobiasRoeddiger/GazePointHeatMap (2018).
121. Shreenath, S. *Implementation of Graph Based Visual Saliency algorithm*, https://github.com/shreelock/gbvs (2019).
122. Jia, S. *EML-NET-Saliency*, https://github.com/SenJia/EML-NET-Saliency/ (2020).
123. Lewin-Koh, J. N. & Bivand, R. Package 'Maptools': Tools for Reading and Handling Spatial Objects, R Package Version 0.8–10, (2011).
124. Obyedkov, I. et al. Saccadic eye movements in different dimensions of schizophrenia and in clinical high-risk state for psychosis. *BMC Psychiatry* **19**, 1–10 (2019).
125. Wolf, A., Ueda, K. & Hirano, Y. Recent updates of eye movement abnormalities in patients with schizophrenia: A scoping review. *Psychiat. Clin. Neurosci.* **75**, 82–100 (2021).
126. Bates, D., Mächler, M., Bolker, B. & Walker, S. Fitting linear mixed-effects models Using lme4. arXiv preprint *arXiv:1406.5823* (2014).
127. Kuznetsova, A., Brockhoff, P. B. & Christensen, R. H. B. lmerTest package: tests in linear mixed effects models. *J. Stat. Softw.* **82**, 1–26 (2017).
128. Marcus, R., Eric, P. & Gabriel, K. R. On closed testing procedures with special reference to ordered analysis of variance. *Biometrika* **63**, 655–660 (1976).
129. Bylinskii, Z., Judd, T., Oliva, A., Torralba, A. & Durand, F. What do different evaluation metrics tell us about saliency models? *IEEE Trans. Pattern Anal. Mach. Intell.* **41**, 740–757 (2018).
130. Judd, T., Ehinger, K., Durand, F. & Torralba, A. Learning to predict where humans look. In *2009 IEEE 12th international conference on computer vision* 2106–2113 (IEEE, 2009).
131. Judd, T, Durand, F. & Torralba, A. A benchmark of computational models of saliency to predict human fixations. (2012).
132. Kümmerer, M., Wallis, T. S. & Bethge, M. Information-theoretic model comparison unifies saliency metrics. *Proc. Natl Acad. Sci.* **112**, 16054–16059 (2015).
133. Borji, A. & Itti, L. A large-scale fixation dataset for boosting saliency research. *arXiv preprint arXiv:1505.03581* (2015).
134. Harel, J., Koch, C. & Perona, P. Graph-based visual saliency. *Adv. Neural Inf. Process Sys.* **19**, 545–552 (2006).
135. Liu, Q., Zhuang, J. & Ma, J. Robust and fast pedestrian detection method for far-infrared automotive driving assistance systems. *Infrared Phys. Technol.* **60**, 288–299 (2013).
136. Jia, S. & Bruce, N. D. Eml-net: An expandable multi-layer network for saliency prediction. *Image Vis. Comput.* **95**, 103887 (2020).
137. Peters, R. J., Iyer, A., Itti, L. & Koch, C. Components of bottom-up gaze allocation in natural images. *Vis. Res.* **45**, 2397–2416 (2005).

ACKNOWLEDGEMENTS

AUTHOR CONTRIBUTIONS

Study design: PA 75%; JH: 5%; DG 20%. Data acquisition: IN 75%; VJ 10%; JJ 5%: VL 5%; PF 5%. Data analysis: PA 70%; LJ 15%; EB 15%. Data interpretation: PA 80%; EB 20%. Writing – original draft preparation: PA 85%; LJ 10%; LJ 5%. Writing – review and editing: JH 45%; LK 15%; VJ 10%; DG 20%; EB 10%.

COMPETING INTERESTS

The authors declare no competing interests.

ADDITIONAL INFORMATION

Supplementary information The online version contains supplementary material available at https://doi.org/10.1038/s41537-024-00438-4.

Correspondence and requests for materials should be addressed to Petr Adámek.

Reprints and permission information is available at http://www.nature.com/reprints

Publisher's note Springer Nature remains neutral with regard to jurisdictional claims in published maps and institutional affiliations.